REGULATION OF MYOSIN IIIA MOTOR/KINASE ACTIVITY

by

Judy Elaine Moore

A dissertation submitted to the faculty of
The University of North Carolina at Charlotte
in partial fulfillment of the requirements
for the degree of Doctor of Philosophy in Biology

Charlotte

2009

Approved by:

_____
Dr. Christopher M. Yengo

_____
Dr. Laura W. Schrum

_____
Dr. Ian Marriott

_____
Dr. Donald Jacobs

_____
Dr. Cynthia Gibas

ABSTRACT

Myosin IIIa, a motor protein that localizes to actin-rich regions of photoreceptors and to stereocilia of inner ear hair cells, is associated with the hearing process in vertebrates and with phototransduction for invertebrates. It contains a large Pak-like kinase domain at its N-terminus that has previously been shown to autophosphorylate residue(s) on the motor domain. We have characterized the autophosphorylation process and its influence on the motor's ATPase activity and actin affinity using a phosphorylated version of our previously developed construct human MIIIa 2IQ, contrasting its activity with the kinase-dead MIIIa 2IQ K50R construct, which has a single substitution mutation in the kinase's catalytic region. We have determined that autophosphorylation is an intermolecular process with rates ranging from ~0.05 min^{-1} to ~0.30 min^{-1} (0.01 - 1.2 µM MIIIa). Although proposed target autophosphorylation sites are near the motor's actin binding region, the autophosphorylation rate is not affected by the presence of actin filaments. We demonstrated that the MIIIa 2IQ ATPase rate in the presence of 20 µM actin decreases over time of pre-incubation with ATP (~40% in 1 h). The ATPase of fully phosphorylated MIIIa 2IQ has lower k_{cat} and higher K_{ATPase} than unphosphorylated MIIIa 2IQ or the K50R construct, while its steady-state actin affinity in the actin co-sedimentation assay (K_{Actin}) is decreased.

We propose that phosphorylation of the myosin IIIa motor by its activated kinase domain reduces the molecule's actin affinity. This concentration-dependent autophosphorylation acts as a downregulatory mechanism that serves to maintain myosin IIIa/cargo concentration at actin bundle tips within physiologically determined limits for maintenance of stereocilia length and flexibility. This model is further supported by

immunolocalization results (Kachar lab, NIH) in which a GFP-tagged version of the kinase-dead construct was demonstrated to localize more effectively to stereocilia tips than GFP-tagged wild type.

ACKNOWLEDGEMENTS

I would like to thank my advisor Dr. Christopher Yengo for his patient and insightful guidance throughout my graduate work. His encouragement, support and high expectations have directed and motivated me to do more than I sometimes felt was possible. Certainly this work would not have been completed without him. I also thank the members of my committee, Dr. Laura Schrum, Dr. Ian Marriott, Dr. Donald Jacobs, and Dr. Cynthia Gibas, for giving of their time and expertise and for their critical evaluation of this manuscript. Additionally, I would like to express my appreciation to members of the UNCC biology graduate faculty their informative, inspirational courses and conversations.

I also thank my colleagues and friends, especially fellow Yengo lab members Darshan Trivedi, Shoba Ananthanarayan, Mingxuan Sun, Kate Hawley, Michael Rose, Niyati Patel, Matthew Draughon and Michael Magnotta for their friendship and assistance.

My husband Jeff has been consistently supportive, encouraging, patient, and calming, and has kept my car running smoothly for all the 157,000 miles these past five years at UNCC have required. For these among many reasons, I am eternally grateful to him.

I also extend thanks to our collaborators, especially Dr. Andrea Dosé of University of California at Berkeley, and Dr. James Sellers and Dr. Bechara Kachar of the National Institutes of Health. This research was funded by National Institutes of Health grant no. EY016419 (C.M.Y.).

TABLE OF CONTENTS

LIST OF TABLES

LIST OF FIGURES

LIST OF ABBREVIATIONS

AM	Actomyosin (included bound nucleotide is AM.ATP or AM.ADP, etc.)
Arr2	Arrestin 2
ATP	adenosine triphosphate
CaM	calmodulin
COS-7	a simian-derived immortal cell line used in research (kidney tubules)
DFNB30	deafness autosomal recessive locus 30
DTT	dithiothreitol
FLAG	a polypeptide protein tag used for myosin purification and antibody recognition, with the sequence N-DYKDDDDK-C
GFP	green fluorescent protein
GMP	guanine monophosphate
HeLa	an immortal cell line used in research (cervical cancer cells)
IQ motif	isoleucine-glutamine rich motif
NADH	nicotinamide adenine dinucleotide
MLCK	myosin light chain kinase
PAK	p-21 activated kinase
PDZ	protein interacting domain
PEP	phosphoenolpyruvate
PIP_3	phosphotidylinositol triphosphate
PK	pyruvate kinase
SDS-PAGE	sodium dodecyl sulfate – polyacrylamide gel electrophoresis
TEDS	a conserved position in myosin motor sequences, occupied by threonine, serine, aspartic acid or glutamic acid

3THDI	myosin III tail homology domain 1
3THDII	myosin III tail homology domain 2
TRPL	toll-like receptor like
WH-2	WASP homology domain-2, ~ 35 residue actin-binding motif

CHAPTER 1: REVIEW OF THE LITERATURE

1.1 The Myosin Superfamily

The myosins are a superfamily of actin-based motor proteins whose individual members perform a wide variety of intracellular functions. All myosins convert chemical energy to mechanical energy by hydrolyzing ATP in an actin-dependent manner. Coordination of the steps in their ATPase cycle with changes in both actin binding affinity and myosin conformation generates force (Sellers 1999), which typically results in translational movement of the myosin motor or of the associated actin filament (Figure 1). Examples of myosin-dependent processes include cellular contraction for cytokinesis or muscular activity, transport of organelles or molecular cargo along actin filament "tracks," and generation of tension for cell motility or other specific cellular processes, including those that contribute to sensory functions.

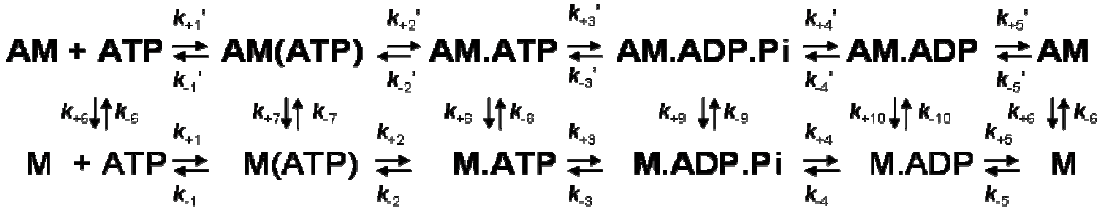

Figure 1. Scheme 1, which describes the actomyosin ATP hydrolysis cycle.

All the myosins have at least three distinct domains: a motor "head," a lever arm "neck," and a rod-like C-terminal tail (Figure 2). The myosin motor is highly conserved, with both nucleotide binding and actin binding regions as well as numerous components

that communicate between these two sites. Relatively small structural variations in this domain for a particular myosin modify the motor's biochemistry, matching its motor characteristics to the myosin's cellular function (De La Cruz and Ostap 2004). The neck domain is called the lever arm because it pivots during the ATPase cycle in order to amplify head movements and magnify force against an actin filament during the hydrolysis cycle. The lever arm's stability is enhanced by the binding of calmodulin or a calmodulin-like light chain at each of its IQ motifs, which range in number from one to six among the known myosins. The myosin tail is its most divergent domain, reflecting the molecule's cellular function according to the specific binding partner(s) with which the particular myosin isoform associates. Examples include vesicular or molecular cargo, membrane components, or filament-forming tail regions of adjacent myosin molecules.

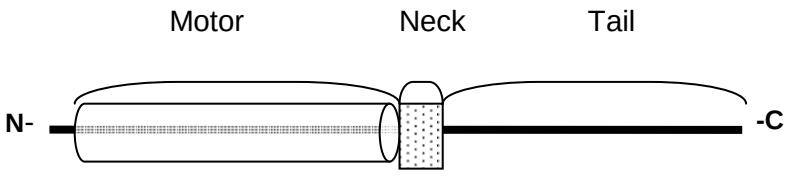

Figure 2. Generalized myosin structure.

There is some variation in the way the myosin superfamily is subdivided, but currently its members are reported to comprise either 24 classes (Foth *et al* 2006) or 35 classes (Odronitz and Kollmar 2007), each including numerous subclasses and isoforms. All eukaryotic species require at least two distinct myosin types and most have nine or more, though no specific class is common to all species (Richards and Cavalier-Smith 2005). Eleven classes have been found in the vertebrates (Foth *et al* 2006). The first identified and most familiar representatives of the myosin superfamily are the muscle myosins, all of which dimerize and assemble into contractile elements called thick filaments. These thick filaments interact with actin-based thin filaments within highly-

ordered contracting structures known as sarcomeres. The filament-forming myosins, both muscle and non-muscle types, make up class II and are known as the "conventional" myosins. The remaining classes, the unconventional myosins, function as either monomers (myosins I and III, for example) or as dimers (myosins V and VI) that move unidirectionally on actin filaments, all with the exception of myosin VI toward the "plus" end. Inactive myosin molecules generally dissociate from the actin filament in the presence of ATP and become free to diffuse unless tethered in place by tail binding. Figure 3 shows an unrooted phylogenetic tree illustrating the relationships among the myosin classes and subclasses based on distance matrix analysis (Clustal-W) using the chicken muscle myosin motor for reference (Dosé *et al* 2003).

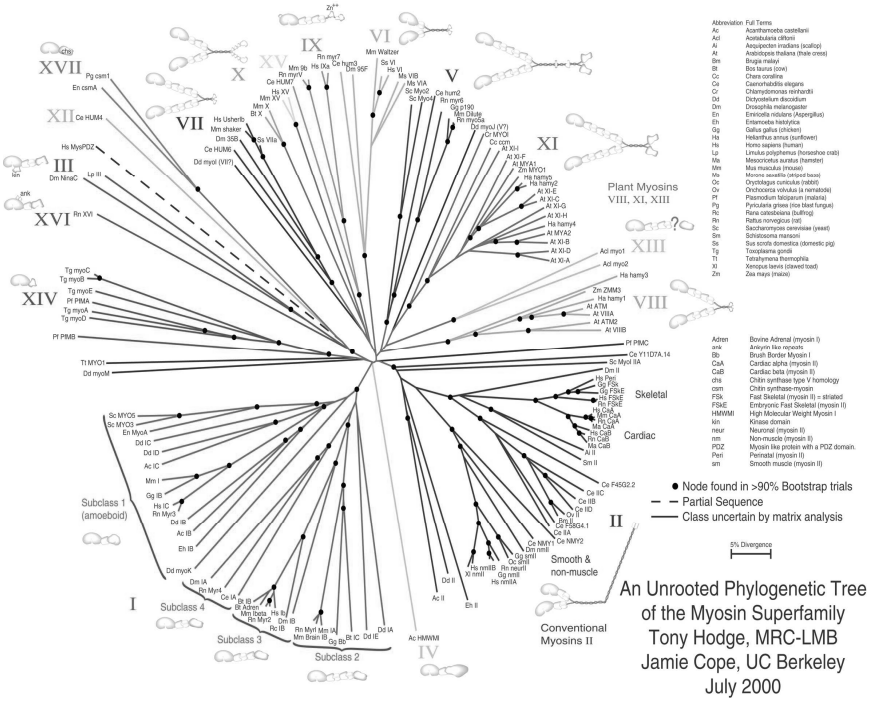

Figure 3. Unrooted phylogenetic tree of myosins, from The Myosin Home Page (Hodge and Cope 2000).

1.2 Class III Myosins

Myosin III was the third myosin class to be identified (Montell and Rubin 1988). It was initially identified from its expression in photoreceptors and in the inner ear

sensory cells (hair cells), where it associates with bundled actin. Myosin III was identified as the gene product of the *ninaC* gene in *Drosophila melanogaster*, so named because of the observation that its deletion results in neither inactivation nor activation of the photoreceptor response (Montell and Rubin 1988). Since then, representatives of the class III myosins have been identified in both invertebrates and vertebrates. The properties of myosin III isoforms from several species in addition to *Drosophila melanogaster* have been investigated, most notably from *Limulus polyphemus* (horseshoe crab), *Morone saxatilis* (striped bass), *Mus musculus* (mouse) and *Homo sapiens* (human). In all known cases except *Limulus* two myosin III isoforms are present, with the longer one designated myosin IIIa (p174 in *Drosophila*) and the shorter myosin IIIb (for *Drosophila*, p132); *Limulus* expresses only the longer isoform. The two isoforms are encoded by separate genes except in *Drosophila* where they are splice variants of a single gene (Montell and Rubin 1988).

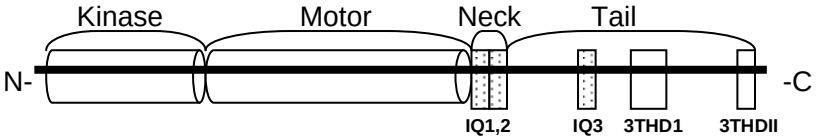

Figure 4. Schematic diagram of myosin IIIa structure.

The class III myosins have unique structural features that distinguish them from other members of the myosin superfamily (Figures 4 and 5). Most notable among these is their N-terminal kinase domain that has been shown to be able to phosphorylate other proteins as well as autophosphorylating the myosin III motor (Ng *et al* 1996, Komaba *et al* 2003). The myosin IIIa motor is relatively divergent, with approximately 25% homology to the class I and class II myosin motors (Cheney *et al* 1993). Our lab has reported the characteristics of the human myosin III motor to include slow steady-state

ATPase activity with high actin concentrations required for full activation, and rate-limiting ADP release as is typical for a high duty ratio motor (Dosé *et al* 2006). Its lever arm has two IQ motifs that bind calmodulin, and its tail includes a third IQ motif and a tail homology domain I (3THD1) that has recently been reported to bind the SH2 domain of the actin bundling protein espin 1, transporting this protein to actin filament tips and thereby contributing to stereocilia elongation (Dosé *et al* 2003, Salles *et al* 2009). The number of IQ motifs in the neck and the tail is quite variable, and both fish and *Limulus* class III myosins have more than the human isoforms (Dosé *et al* 2003). Human myosin IIIa but not IIIb also has a tail homology domain II (3THDII) that includes an actin binding motif proposed to contribute to processive movement along actin filaments. Neither isoform appears to have a sufficient coiled coil-forming region to dimerize, so it is most likely a one-headed myosin (Dosé *et al* 2003). There is greater sequence homology among the known myosin IIIa isoforms of different vertebrate species than between the IIIa and IIIb sequences within the same species (Katti *et al* 2009).

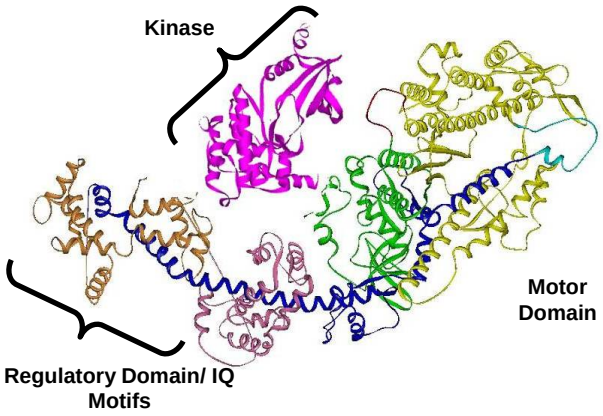

Figure 5. Ribbon diagram of proposed structure of myosin III kinase, motor and lever arm domains.

Class III myosins appear to be exclusive to photoreceptors in *Drosophila* and *Limulus*, and are also highly expressed in vertebrate retinal tissues and inner ear sensory receptor cells. Vertebrate myosin III transcripts are detectable in brain, kidney, testes,

intestine and pancreatic tissue as well. However, for both bass myosin IIIa and IIIb, transcription levels are reported to be considerably lower in the non-sensory tissues (ten to fifty times lower for myosin IIIa, two to four times lower for IIIb) (Dosé *et al* 2000, Dosé *et al* 2003). Specific functions for class III myosins in non-sensory tissues are as yet undetermined (Dosé *et al* 2000, Dosé *et al* 2003, Katti *et al* 2009). In fish, both myosin III isoforms are present at the photoreceptors but only MIIIa transcript expression has been detected in the cochlea (Dosé *et al* 2003, Walsh *et al* 2002). The consensus of numerous studies over more than a decade is that class III myosins play important roles in several aspects of hearing and vision, but there is much that remains to be determined.

1.3 Myosin IIIa and Vision

The visual process has been extensively investigated in *Drosophila* photoreceptors, which have the fastest G protein-coupled signaling cascade yet identified. Both vertebrate and invertebrate photoreceptors are highly polarized cells with a cell body and a signaling compartment called either the outer segment (vertebrate) or the rhabdomere (invertebrate) (Figures 6 and 7). The signaling compartment houses the major proteins essential for phototransduction and either contains stacked membranous discs (vertebrates) or has thousands of microvilli in a comb-like arrangement down one side (invertebrates). In this compartment photon

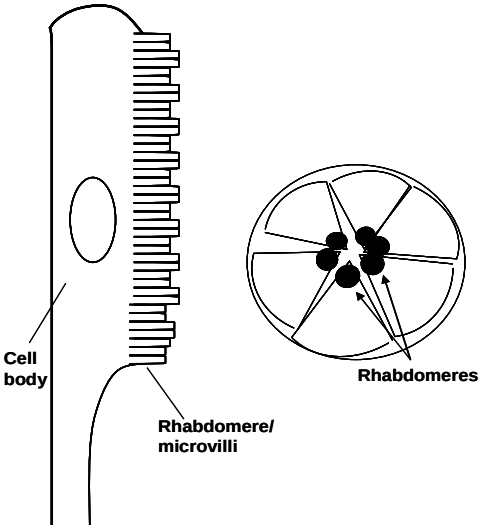

Figure 6. A single invertebrate photoreceptor cell with its rhabdomere, left. At right is a transverse section of one ommatidia, showing the orientation of rhabdomeres.

absorption by the photopigment rhodopsin activates a G protein ($G_q\alpha$ for *Drosophila*, transducin for vertebrates) to initiate a sequence of events that results in activation (deactivation in the vertebrate system) of the light sensitive ion channels TRP and TRPL. Reversal of the response involves inactivation of the photopigment by its binding with arrestin2 and interaction with Ca^{++}.

It has been established that several of these key signaling proteins undergo light-dependent translocations into and out of the signaling compartment, a shuttling that appears to be essential for adjusting both sensitivity and speed of the photoresponse. Altering the concentration of signaling proteins is an adaptive response to the broad range of light intensities within which photoreceptors function. The Gα and β subunits and TRPL cation channels are concentrated in the signaling compartment in dark-adapted animals but approximately fifty percent of each of these proteins shuttles to the inner segment/cell body over the course of several minutes of light exposure. Visual arrestin1 and arrestin2 translocate in the opposite direction upon light exposure, from the cell body or inner segment into the outer segment/rhabdomere where they participate in response termination.

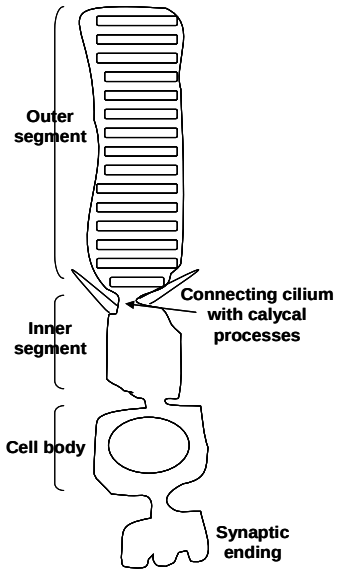

Figure 7. Vertebrate photoreceptor (rod).

In both vertebrate and invertebrate photoreceptors myosin III is heavily associated with areas rich in bundled actin filaments (Diagrams 6 and 7), particularly between the cell body/inner segment and the rhabdomere/outer segment. This region's bundled actin filaments are directionally organized so that their plus ends are oriented either

toward the signaling compartment or, for vertebrates, are contained within microvilli-like structures called calycal processes that project from the base of the outer segment of vertebrate photoreceptors. Their minus ends extend into the cell body/inner segment (vertebrates) or even beyond into the myoid region (Nagle *et al* 1986). Null mutants of the *ninaC* gene products undergo light-induced degeneration of the retina and disruption of the actin cytoskeleton, which suggest that these gene products are needed for cell maintenance (Matsumoto *et al* 1987). The *Drosophila* isoforms are differentially localized, with p174 contained within the rhabdomeres and p132 in the cell bodies of photoreceptors (Porter *et al* 2002). Fish myosin IIIa is heavily concentrated at the tips of calycal processes and is also present in the actin-rich regions of the inner segment, while myosin IIIb has been visualized as having a more generalized distribution in these regions as well as the outer segment (Dosé *et al* 2003, Lin-Jones *et al* 2009). Immunolocalization studies revealed that fish myosin IIIa is abundant in the retinal pigmented epithelium, while IIIb was detected in the retina's outer limiting membrane, which is formed by actin-containing projections from the glial Müller cells (Lin-Jones *et al* 2009). A similar differential distribution has very recently been reported for mouse myosin IIIa and IIIb (Katti *et al* 2009).

1.4 Roles of Class III Myosins at Invertebrate Photoreceptors

Several lines of evidence have implicated both of the *Drosophila ninaC* gene products (myosin III isoforms p174 and p132) in the visual process. The p174 isoform is essential for response termination (Porter *et al* 1992), and while both isoforms influence long-term adaptation to changes in light intensity, p132 in particular is needed for a normal response (Lee and Montell 2004). Arrestin is the photoreceptor protein that

initiates termination of the light signal by binding to photoexcited and phosphorylated rhodopsin. Arrestin translocates from the cell body into the rhabdomere as light exposure excites increasing quantities of rhodopsin, consequently requiring more and more arrestin for adequate quenching (Peet *et al* 2004). The light-dependent translocation of visual arrestin2 was shown to be based on the binding of Arr2 to phosphoinositide (PIP_3)-enriched vesicles, and evidence has been presented implicating myosin IIIp132 as the Arr2 transporter via a tail linkage to (PIP_3)-enriched vesicles (Lee and Montell 2004). However, this requirement for NINAC has been more recently challenged by Satoh and Ready (2005), who did not find a NINAC (myosin III) requirement for translocation of either arrestin1 or arrestin2 (Satoh and Ready 2005). The light-dependent process is complete within ten minutes, while the retrograde movement of Arr2 that reestablishes resting conditions requires several hours and has been attributed to diffusion rather than myosin motor activity (Lee and Montell 2004).

A light-instigated shift of much of the $G_q\alpha$ from the *Drosophila* rhabdomere to the cell body takes place within five minutes of continuous illumination and is dependent on light intensity, while in darkness the translocated $G_q\alpha$ returns to the rhabdomeres. These compartment shifts are essential for long-term adaptation to light intensity. $G_q\alpha$'s rapid exit from rhabdomeres is dependent on rhodopsin activation by light but does not require NINAC protein nor any of the downstream signaling components investigated (Cronin *et al* 2004) and is independent of arrestin or TRPL channel movements (Cronin *et al* 2004). However, $G_q\alpha$'s normal rate of return to the rhabdomeres does appear to involve myosin III, yet because it will slowly take place even in the absence of myosin III it may be that diffusion plays a role as well (Cronin *et al* 2004). The authors point out that because

myosin III is both a motor protein and a functional kinase, it is possible that $G_q\alpha$ transport may depend upon its kinase activity rather than motor function (Cronin *et al* 2004). While vertebrate myosin III has been demonstrated to exhibit motor activity in the *in vitro* sliding assay (Komaba *et al* 2003), and movement into the rhabdomere is in the expected direction for a plus-end directed motor, there has not yet been direct verification of mechanoenzymatic activity for the invertebrate myosin IIIs. It has been suggested that the lack of a critical salt bridge in the invertebrate motor may prevent motor activity, and that myosin III's function in *Limulus* may be as an actin binding protein (Kempler *et al* 2007).

Drosophila myosin III is capable of concentrating calmodulin (CaM) in the rhabdomere, which it can bind not only by lever arm IQ motifs but also by its multiple tail domain IQ motifs (Porter and Montell 1993). It has been proposed that calmodulin transport gives p172 an indirect role in Ca^{++} dependent metarhodopsin inactivation, essential to the termination of the light response. Calmodulin may act as an intermediate that responds to calcium influx by accelerating the rate of arrestin binding to metarhodopsin (Liu *et al* 2008). Recent studies indicated that the Ca^{++} dependence did not depend on rhodopsin dephosphorylation when normal calmodulin was present, but when Ca^{++} was present rhodopsin could not be inactivated in the presence of mutant calmodulin nor of NINAC mutants (Liu *et al* 2008). The authors suggest a mechanism whereby CaM and NINAC mediate localized Ca^{++} influx in the rhabdomere, which accelerates the binding of arrestin to activated metarhodopsin and is said to promote high efficiency, temporal resolution and fidelity of the signaling process (Liu *et al* 2008).

Studies investigating the light-induced translocation of TRPL channels from rhabdomere to cell body have revealed that this is dependent on calcium influx through the Ca^{++} specific TRP gated channels, and is an important component of reduced photosensitivity under bright light conditions. Activation of very low (<1%) levels of rhodopsin and $G_q\alpha$ trigger the translocation (Liu *et al* 2008). A NINAC mutant showed partially compromised TRPL-eGFP rhabdomeric recovery in the dark, but this has been attributed to secondary effects of the mutation, particularly its disrupted actin cytoskeleton and retinal degeneration (Meyer *et al* 2006, Matsumoto *et al* 1987). Because TRPL is a transmembrane protein it cannot be solubilized and thus its translocation is expected to require an endocytotic pathway (Meyers *et al* 2006).

The signalplex, a large assembly of many of the proteins critical for *Drosophila* phototransduction (TRP channels, rhodopsin, phospholipase C, protein kinase C, and G protein coupled receptors), localizes to the rhabdomere and is assembled by the PDZ-domain scaffolding protein INAD (Wes *et al* 1999). It was demonstrated that INAD binds directly to NINAC, and disruption of the interaction slows the termination of the photoresponse although it does not affect NINAC localization (Wes *et al* 1999). The role played by myosin III as a component of the signalplex remains to be determined.

The *Limulus* myosin III in lateral compound eyes localizes to rhabdomeres, where it undergoes phosphorylation changes in concert with circadian rhythms (Edwards and Battelle 1987; Cardasis *et al* 2007). There are numerous structural and functional changes that take place in these photoreceptors in association with the light-dark cycle, and myosin III phosphorylation status may mediate some of these changes (Kempler *et al* 2007). Phosphorylation of certain target residues may influence actin affinity, and it is

suggested that changes in phosphorylation status may "prime" the lateral eye photoreceptor to undergo transient membrane shedding from the microvilli of the rhabdomere (Cardasis *et al* 2007).

1.5 Roles of Class III Myosins in Vertebrate Vision

The functional processes of vertebrate photoreceptors are similar in a general way to invertebrates. Rhodopsin is activated by light, activating the G protein subunit transducin α which induces the photoresponse, which is accomplished by stimulating cGMP phosphodiesterase to rapidly reduce intracellular cGMP and close the gated cation channel in the plasma membrane. The events of rapid recovery from the photoresponse are also similar, involving phosphorylation of photoexcited rhodopsin and subsequent arrestin binding, with regulation of rhodopsin kinase activity by a calcium binding protein. As described for invertebrates, key vertebrate signaling proteins also undergo massive intracellular translocation for adaptation. Calvert *et al* (2006) estimated the rates of diffusive equilibrium in the outer segment, inner segment and connecting cilium of rods, and concluded that diffusion may successfully explain the light-initiated translocation of both transducin and arrestin without assistance from a motor bound transport. Currently the dark adaptation mechanism for returning transducin and/or arrestin to their inactive concentrations in each compartment is not well enough understood to allow potential roles to be distinguished between molecular motors and/or diffusion in these processes (Calvert *et al* 2006). Fish myosin IIIa transgenic expression in *Xenopus laevis* rod photoreceptors resulted in abnormally large actin filament bundles in the calycal processes, which was interpreted as suggestive of a role for myosin IIIa in

the morphogenesis and maintenance of actin bundles, perhaps in addition to other functions related to cytoplasmic transport and/or signaling (Lin-Jones *et al* 2004).

1.6 Myosin IIIA and Human Hearing

A naturally occurring set of three mutations in the human myosin IIIa gene has been designated as the nonsyndromic progressive recessive form of deafness DFNB30, which has no known corresponding visual or balance defect (Walsh *et al*, 2002). DFNB30 was described in three generations of an Israeli family of Iraqi descent, who experience bilateral hearing loss that progresses from reduced high-frequency hearing in the second decade to severe hearing loss by age fifty (Walsh *et al*, 2002). Three mutations within the myosin IIIa gene were identified in the affected family members. The earliest age of onset along with significantly poorer hearing during the progressive stages were associated with homozygosity of a nonsense mutation, a single substitution in exon 28 in codon 1043 (3126T→G) resulting in a premature stop codon that truncates the protein at its head/neck junction (Walsh *et al*, 2002). The other two mutations were localized to the splice acceptor sites of intron 17 and intron 8, one resulting in deletion of exon 18 in the motor domain and the other producing an unstable message so that expression is significantly reduced (Walsh *et al*, 2002). All homozygotes for any of these mutations eventually developed deafness of equal severity by the sixth decade, while simple heterozygotes were unaffected (Walsh *et al*, 2002). This investigation within a single family demonstrated that myosin IIIa is required for normal hearing and suggested that other mutations in this gene may also exist, perhaps some that affect both vision and hearing as reported for myosin VIIa in the disease Usher 1b (Walsh *et al*, 2002; Petit *et al*, 2001 review).

The discovery of DFNB30 has resulted in the recent myosin IIIa research focus on its role in the inner ear sensory receptor cells (Figure 8). It has been shown to associate with the actin bundle cores of stereocilia, the highly specialized microvilli on the apical surface of inner ear hair cells that contain mechanoresponsive cation channels. Myosin IIIa localizes to the tips of filopodia in HeLa and COS-7 cells (Dosé *et al* 2007; Salles *et al* 2009), and the same GFP-tagged construct has been found to localize to a previously unidentified compartment at the tips of stereocilia on inner ear hair cells (Schneider *et al* 2007). It was recently shown to colocalize with the actin bundling protein espin I at stereocilia tips, and the combined overexpression of both myosin IIIa and espin I resulted in more stereocilia elongation than over expression of either alone, an effect that was even more pronounced in filopodia of COS-7 cells (Salles *et al* 2009).

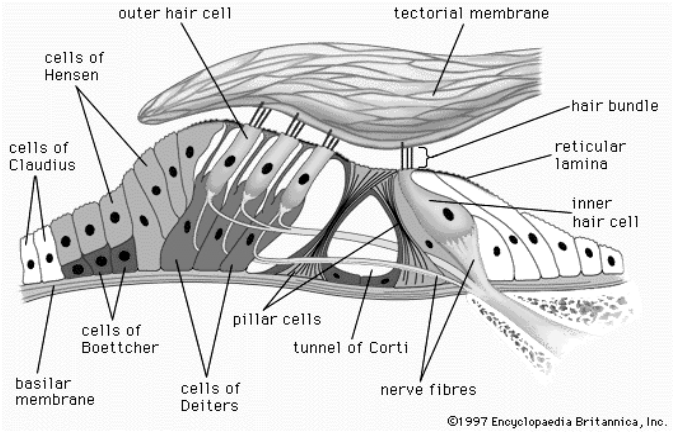

Figure 8. Cochlea cross section showing the position and appearance of rows of outer and inner hair cells in organ of Corti. *(Encyclopedia Britannica, 1997)*

The sensory tissues of the auditory epithelium are said to be "the most precisely and minutely engineered tissues of the body" (Alberts *et al* 2002). The hair cells of this epithelium have elongated mechanosensory protrusions on their apical surfaces called stereocilia, which are organized precisely into staircased rows, with each one attached to the adjacent taller one by a fibrous tip link (Figure 9). These cells respond to auditory stimuli by triggering a receptor potential called the MET (mechanoelectrical transduction) current when their

stereocilia are perturbed by endolymph fluid vibrations. Not only are stereocilia lengths regulated according to row on an individual hair cell, but also there is a gradual decrease in length around the two and a half turns of the cochlea from its base to its apex, sensitizing different regions of the organ of Corti to vibrations of different frequencies. Stereocilia are highly specialized microvilli and so have bundled parallel actin filaments at their core, with the plus ends of the filaments oriented toward the tip. These bundles are continually renewed by a treadmilling process in which they add new actin monomers as well as actin bundling proteins at their tips and remove "old" ones from their base, and yet continuously maintain their precise lengths and functionality. Not surprisingly stereocilia have numerous myosin isoforms in association with them. At least six of these, including myosin IIIa, are known to be essential to the hearing process, either directly during response to a stimulus or indirectly as a component of maintenance or regulatory processes, and have been demonstrated to be associated with specific hearing disorders when mutated (Redowicz 2002 review, Friedman *et al* 2007 review). (see Figure 9). Each stereocilium's length, flexibility, and intracellular and transmembrane components must be carefully regulated and maintained for a lifetime in order for these terminally differentiated cells to remain functional. Elucidating the role played by specific myosins

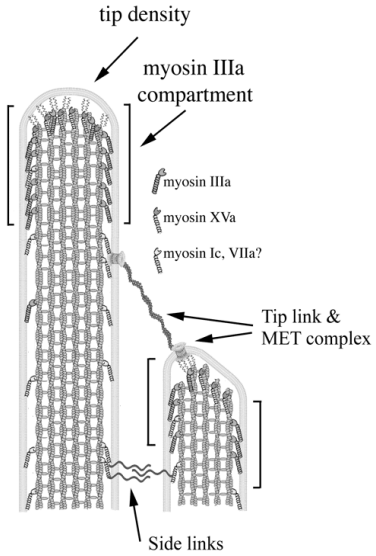

Figure 9. Stereocilia with representative associated myosins, MET complex and tip links. *(Schneider et al. 2006)*

is essential to understanding the hearing process at the molecular level, as well as for the eventual development of treatments to reverse myosin-related hearing defects.

Developmentally, the appearance of detectable levels of myosin IIIa in stereocilia is associated with the maturation of actin bundle structure and also coincides with or closely precedes the onset of MET currents (Waguespack *et al* 2007), suggesting a role in transporting components either of the MET machinery or of the stereociliary structure. Myosin IIIa encloses the tip of the actin bundle in a thimble-like pattern, distinct from the distribution pattern of other myosins of the stereocilia (Schneider *et al* 2006). Localization requires the motor domain but not the actin-binding motif of the tail 3THDII domain, and deletion of the kinase domain results in both stereocilia elongation and bulging of the tip compartment occupied by myosin IIIa (Schneider *et al* 2006). This compartment encompasses both the region of the MET machinery and the site of actin polymerization, suggesting that myosin IIIa may participate in either or both of these processes. Similar colocalization of myosin IIIa and the actin bundling protein espin 1 was observed. Overexpression of either of these two proteins is associated with stereocilia elongation, while overexpression of both causes greater elongation (Salles et al 2009). The myosin IIIa 3THD1 domain associates with the WH-2 motif of espin 1 (Salles *et al* 2009). These results indicate that at least one function for myosin IIIa is the transport of espin 1 to stereocilia tips, but do not preclude the possibility of other roles as well, perhaps transport of MET components in an analogous function to what has been observed in *Drosophila* photoreceptors (Salles *et al* 2009).

1.7 Potential Partial Overlap in Myosin IIIA and IIIB Function

While discovery of the human myosin IIIa mutations that are causative for the DFNB30 deafness phenotype has spurred investigations to elucidate its role in the hearing process, it also raises questions about the lack of a visual component in this disease, especially given myosin IIIa's importance for *Drosophila* vision. It has been hypothesized that a redundancy of function exists in vertebrate photoreceptors, so that perhaps the similarities between myosin IIIa and myosin IIIb structure, in conjunction with their overlap in localization and function may provide an explanation. Two recently published reports describe localization studies for myosin isoforms in the eye, one in fish and the other in mice (Lin-Jones *et al* 2009; Katti *et al* 2009). Both show partial overlap of myosin IIIa and myosin IIIb localization, most notably at the actin-rich distal portion of the inner segment (Lin-Jones *et al* 2009; Katti *et al* 2009). Further studies are required to confirm whether this localization overlap actually translates to a redundancy of function sufficient to overcome the myosin IIIa deficiency associated with DFNB30.

1.8 Regulation of Myosin IIIA Motor Activity

The regulation of myosin motor activity is crucial to its cellular functionality, and any explanation of the myosin's cellular role is incomplete without a determination of how it is regulated. In order for myosin IIIa to be able to maintain proper stereocilia lengths it must transport the necessary amount of espin I to be incorporated at their actin bundle tips. A kinase-deleted construct developed in our lab (MIIIa 2IQ ΔK) has been demonstrated to have a higher maximum rate of ATPase activity and stronger actin affinity than the comparable construct containing the kinase domain (MIIIa 2IQ) (Dosé *et*

al 2006, Dosé *et al* 2008). Compared to MIIIa 2IQ, it localizes more effectively to actin bundle tips in filopodia and stereocilia while simultaneously elongating them (Dosé *et al*, 2006; Salles *et al* 2009). This suggests that the myosin IIIa kinase domain is involved in downregulation of function by influencing the activity of its motor.

Mechanisms for regulating myosin activity to maintain proper cellular functioning have not yet been elucidated for many of the unconventional members of the myosin superfamily, but phosphorylation and dephosphorylation are among known myosin regulatory processes that also include calcium binding and availability of cargo. For the conventional myosins, calcium's role in the tight regulation of motor activity has been investigated extensively. The stimulus for contraction in cardiac and skeletal muscle results in sudden calcium influx in the vicinity of the contractile apparatus, calcium binding to the thin (actin/troponin/tropomyosin) filament and subsequent induction of a structural change that allows actomyosin cycling to begin (Huxley 1971, Vibert *et al* 1997). For smooth muscle myosin and the non-muscle class II myosins, calcium influx results in myosin light chain kinase (MLCK) activation, phosphorylation of the myosin regulatory light chain by activated MLCK and subsequent motor conformational change to an active state (Trybus *et al* 1994). Cessation of the stimulus prevents further activity by various means involving dephosphorylation of the light chain, calcium removal, and motor/tail phosphorylation (Trybus *et al* 1994).

Much less is known about regulation of unconventional myosin activity, but it appears to be accomplished by several means. Myosin V motor regulation has been reported to involve calcium concentration influences on both calmodulin light chain binding and tail-motor interactions (Krementsov *et al* 2004, Lu *et al* 2006) as well as

cargo binding to the globular tail domain (Olivares *et al* 2006). The calcium dependent structural changes are characterized by an extended, active conformation and a conformation that is inactive and folded, in which the myosin V globular tail domain blocks the motor's active site (Krementsov *et al* 2004). Tail-motor interactions may regulate myosin VII activity as well (Umeki *et al* 2009). For many myosin I isoforms, motor phosphorylation of a serine or threonine residue at the highly conserved TEDS site (the amino acid residue must be a phosphorylatable threonine or serine, or an acidic glutamic or aspartic acid) on a surface loop of the actin binding region has been shown to upregulate motor activity (Bement and Mooseker 1995 review; Brzeska and Korn 1996; Redowicz 2001 review). In myosin VI the role of phosphorylation at the TEDS site's threonine residue is less clear, but in addition to calcium concentration it may influence the motor's kinetic properties (De La Cruz *et al* 2001; Morris *et al* 2003; reviewed in Buss and Kendrick-Jones 2009).

Motor phosphorylation of human myosin IIIa is not at the TEDS site but rather has been determined by limited chymotrypsin proteolysis to be within a 20 kDa peptide at the C-terminal end of the motor (Komaba *et al*, 2003). Recent studies of *Limulus* myosin IIIa, which is found in photoreceptors of lateral eyes where its phosphorylation is associated with increased retinal sensitivity at night, indicate that autophosphorylation of this myosin takes place at several sites within and near loop 2, an important actin binding region that partially overlaps with the 20 kDa peptide region identified by Komaba (Kempler et al 2007). Studies involving selective point mutations in the loop 2 sequence have revealed that, for myosin II motors, loop 2 influences both actin affinity and phosphate release (Uyeda *et al*, 1994; Murphy and Spudich, 1999), while in myosin V it

apparently is important for allowing actin binding during the relatively weak binding states (Yengo and Sweeney 2005). Actin affinity has been found to increase with increasing loop 2 net positive charge (Joel *et al* 2003), so the charge reduction associated with loop 2 phosphorylation may be expected to decrease actin affinity.

1.9 Characteristics of the Myosin IIIA Kinase

The myosin III kinase has greatest sequence homology to the catalytic region of the p21 activated kinases, specifically the Pak1 and Ste20 kinase groups (Sells and Chernoff 1997; Dosé *et al* 2003). This family of serine-threonine kinases includes those that phosphorylate the TEDS sites of amoeboid myosin I and myosin VI for activation and those that are important in regulating polymerization of the actin cytoskeleton (Daniels and Bokoch 1999). The Pak kinases are themselves regulated by phosphorylation, with a highly conserved activation target residue in the catalytic site. Although most also include a phosphorylatable regulatory domain, the myosin IIIa kinase does not (Parrini *et al*. 2002).

Pak kinases are “basophilic kinases” in that they preferentially phosphorylate substrates that have basic residues near the phosphorylation site, due to interactions with two acidic residues that create a negatively-charged pocket in the kinase’s major groove. (Ghu *et al* 2005). Each basophilic kinase family appears to prefer basic residues in a different set of positions around the target serine or threonine (Ghu *et al* 2005). The Pak1 kinases are distinguished by an exceptionally strong preference for arginine in the target residue’s “P -2” position. They also share a strong preference for arginine at “P -5,” and also favor arginine at “P -3” and “P -4,” (negative number indicates the position of the basic residue upstream (N-terminal) from the phosphorylation target) (Zhu *et al* 2005,

Rennefahrt *et al* 2007). Specificity profiling of selected Pak1 kinases was used to develop position specific scoring matrices (PSSM) of neighboring residues around known phosphorylation targets, and substrate specificity was found to be virtually indistinguishable among the kinases of the Pak1 family (Rennefahrt *et al* 2007). It is suggested that this research group's Pak PSSM along with the Internet-based Scansite tool can be used as a mechanism for prioritizing direct testing of potential target residues in a putative substrate (Rennefahrt *et al* 2007). This technique may be useful in the process of identifying specific autophosphorylatable target threonines and/or serines in the myosin IIIa molecule.

Based on the current understanding of myosin IIIa function in inner ear hair cells, it is evident that myosin regulatory activity is necessary in order to maintain stereocilia at the appropriate length with proper bundling of their actin core. It has been demonstrated that the myosin IIIa cargo, the actin bundling protein espin I, is incorporated into the actin bundle solely at its tip, which contains the plus ends of its component parallel filaments (Salles *et al* 2009). Excessively long stereocilia and filopodia have resulted from transfection of either exogenous myosin IIIa or espin I, and markedly so when the two proteins were cotransfected, while stereocilia were short and non-functional when espin I was lacking (Schneider *et al* 2006, Salles *et al* 2009, Zheng L *et al* 2000.; Rzadzinska *et al* 2002). Transfection of kinase-deleted myosin IIIa or to a lesser extent, kinase-dead, results in its increased accumulation at actin bundle tips along with elongation and reduced rigidity of the actin bundle (Dosé *et al* 2006, Schneider *et al* 2006, Salles *et al* 2009).

1.11 Hypothesis

These studies provide support for a general hypothesis that myosin IIIa motor activity may be down-regulated by autophosphorylation in a manner consistent with a negative feedback mechanism. This regulatory mechanism would allow the myosin IIIa - espin I system to maintain each stereocilium at the length appropriate for its proper response to fluid vibrations of its targeted frequency and magnitude. We propose that the dual kinase-motor structure of myosin III and the preference of the kinase domain to autophosphorylate the motor in an intermolecular manner provide a mechanism for self-regulation of myosin III concentration as it accumulates at the tips of actin bundles. The bulging stereocilia or filopodia tips characteristic of cells transfected with kinase-deleted MIIIa-GFP suggest that myosin molecules travel to the plus ends of the actin filament bundle and remain attached upon arrival in the tip compartment, lacking a mechanism for turning the motor off and/or for reducing their actin affinity. The kinase deleted construct's high steady-state ATPase rate and high actin affinity relative to wild type also support the concept that this is an unregulated motor. The kinase-dead construct, which has only a single substitution mutation rendering it unable to autophosphorylate its motor, also accumulates at actin bundle tips and elongates filopodia beyond the levels observed for wild type transfections. We suggest that this accumulation is due to the lack of a down-regulatory effect on the motor from autophosphorylation, and that maintenance of actin bundle lengths is dependent upon the concentration of myosin IIIa in the tip compartment. The differences observed between kinase-dead and kinase-deleted myosin IIIa may be attributable to structural interactions between the kinase and the motor.

Specifically we hypothesized that the autophosphorylation processes responsible for both activating the kinase domain and phosphorylating the motor domain of myosin IIIa are concentration dependent and can take place in the presence of actin filaments. Further, when the kinase domain is active it is capable of autophosphorylating the motor domain in the loop 2 region by an intermolecular process, thereby reducing the motor's activity and actin affinity. We tested this hypothesis by monitoring the rate of autophosphorylation across a series of myosin concentrations and in the presence as compared to the absence of actin filaments. Furthermore, we measured the steady state enzymatic activity and actin affinity of a fully-phosphorylated myosin IIIa, in comparison to both an unphosphorylated control and a kinase dead myosin IIIa construct. We report herein results that show phosphorylation to reduce the activity of the myosin IIIa motor and to reduce its actin affinity. In addition, the lack of motor phosphorylation is associated with higher actin affinity. We also report findings that indicate autophosphorylation rates are directly proportional to myosin concentration, consistent with autophosphorylation as an intermolecular process. Our results suggest that levels of phosphorylated myosin are adjusted according to the concentration of myosin present.

Because the negative charge associated with phosphorylation of target residues in critical regions of the motor has the potential to reduce actin affinity and/or rate of product release, autophosphorylation may serve to down regulate myosin IIIa motor activity. Our comparison of phosphorylated and unphosphorylated myosin IIIa constructs in steady-state ATPase and actin binding assays provide further support for our model of myosin IIIa down-regulation of motor activity by autophosphorylation as a mechanism for maintenance of actin bundles in stereocilia. We show *in vitro* evidence

that autophosphorylation is not hindered by the presence of actin filaments, so it is reasonable to suppose that the myosin motor can be phosphorylated *in vivo* as well. This work contributes to our overall understanding of maintenance of the hearing response at a fundamental level. As structural, biochemical, and cell biological roles of the various myosins and other proteins essential to the visual and auditory processes are elucidated the groundwork will be laid for a better understanding of how disruptions in their genes contribute to sensory disorders. Knowledge of the role of myosins in sensory cells interactions may serve as a basis for future development of treatments for visual and hearing-related disorders.

CHAPTER 2: INTRODUCTION

Myosin IIIa, an unconventional myosin localized to the calycal processes of photoreceptors and the stereocilia of the inner ear, is unique among members of the myosin superfamily in that its structure includes an N-terminal domain with serine-threonine kinase activity (Dosé and Burnside, 2000; Komaba *et al*, 2003). This domain is similar to the catalytic domain of the Pak1 kinases and is capable of autophosphorylating site(s) at the C-terminal end of the myosin IIIa motor domain (Komaba *et al*, 2003). The lever arm of myosin IIIa contains two isoleucine-glutamine rich IQ motifs which bind calmodulin or myosin light chains. Typically the structure of the tail region for a specific class and subclass of myosin reflects its unique role in the cell, and in myosin IIIa it includes a third IQ motif, the myosin tail homology 1 motif (3THDI), and the tail homology II actin-binding motif (3THDII) near its C-terminus. Because there is no evidence of a coiled-coil forming region myosin IIIa is presumed to be a single-headed myosin. Human myosin IIIa has demonstrated both ATPase activity and the ability to move actin filaments *in vitro*, consistent with the characteristics of a cellular transporter or force transducer (Komaba *et al*, 2003; Dosé *et al*, 2007; Kambara *et al*, 2006; Dosé *et al*, 2008).

Myosins couple ATP hydrolysis with changes in both conformation and actin binding affinity in order to cyclically generate mechanical force along actin filaments. Small differences among myosin motor domains result in properties finely-tuned for a

specific myosin's biological role in the cell (Holmes and Geeves, 1999). Additionally, motor function may be regulated intracellularly by variation in factors such as calcium concentration, presence or absence of cargo, and/or phosphorylation of the heavy chain's motor or tail, or on light chains (Sellers, 1999; Krementsov *et al*, 2004; Thirumurugan *et al*, 2006). It is postulated that autophosphorylation of the myosin IIIa motor may act as a means for its regulation in photoreceptors and inner ear hair cells under specific cellular conditions (Ng *et al*, 1996, Dosé *et al*, 2008).

The particular cellular functions of myosin IIIa are currently under active investigation. It is known to be localized within the photoreceptors of invertebrates as well as vertebrate sensory receptor cells of the retina and cochlea. It was first identified in *Drosophila* photoreceptors as the *ninaC* gene product (neither inactivating nor activating) that, when deleted, was associated with abnormal retinal electrophysiological response and retinal degeneration (Montell and Rubin, 2088). NINAC was demonstrated to require the motor but not the kinase domain in order to localize at the actin-bundle filled rhabdomere, a structure that is the primary site of phototransduction activity and thus is analogous to the vertebrate outer segment (Porter and Montell, 1993). Other studies have demonstrated its ability to localize at the tips of actin bundles in photoreceptors of bass (Dosé *et al*, 2003) and *Xenopus* (Lin-Jones *et al*, 2004), as well as inner ear hair cell stereocilia of mice (Schneider *et al*, 2006) and filopodial tips in HeLa cells (Dosé *et al*, 2008). Two isoforms designated myosin IIIa and IIIb have been identified in vertebrates (Dosé and Burnside, 2003, Dosé *et al*, 2003), and disruption of the human myosin IIIa gene has been associated with the development of non-syndromic deafness DFNB30 (Walsh *et al*, 2002; Vreugde *et al*, 2003).

Previous studies have indicated that actin bundle tip localization of myosin IIIa in filopodia and in stereocilia of inner ear hair cells is enhanced by removal of the myosin IIIA kinase domain (Dosé et al, 2008, Schneider *et al*, 2006). A previously unknown compartment at stereocilia tips was found to expand in mouse cochleae transfected with kinase-deleted myosin IIIa (Schneider *et al*, 2006). This suggests that myosin IIIa may perform an essential role at stereocilia tips, with a potential regulatory function for the myosin IIIa kinase. Recently we have reported that myosin IIIa via its 3THD1 tail motif binds to the stereocilia-specific actin bundling protein espin I via its WH2 domain, myosin IIIa and espin I colocalize at stereocilia tips of mouse inner ear hair cells and the filopodia tips of COS-7 cells, and that their cotransfection results in both stereocilia lengthening and a remarkable 10-fold lengthening of the filopodia (Salles *et al* 2009). While it is possible that myosin IIIa may transport essential components of the phototransduction pathway in *Drosophila* photoreceptors (Porter *et al*, 1993; Lee and Montell, 2004; Cronin *et al*, 2004), parallel functions have not been elucidated in the vertebrate eye.

Our lab previously has reported kinetic analyses of myosin IIIa constructs truncated after the second IQ domain, with and without the kinase domain, designated myosin IIIa 2IQ and myosin IIIa 2IQ Δkinase (Dosé *et al*, 2006; Dosé *et al*, 2008). Notable differences between the two constructs were found in steady state and transient kinetics as well as degree of filopodia tip localization. The actin-activated ATPase assay for the kinase-deleted construct (MIIIa 2IQ ΔK) showed a two-fold higher k_{cat} and five-fold lower K_{ATPase} than MIIIa 2IQ, as well as five-fold higher steady-state actin affinity. The rate-limiting step for MIIIa 2IQ was modeled to be a transition between two

AM.ADP states, while the faster MIIIa 2IQ ΔK exhibited slow, rate-limiting ATP hydrolysis. Another lab has recently reported similar results for a motor-only construct (Kambara *et al*, 2006), with differences that may be attributed to their removal of the lever arm and lower salt concentrations in assays (Dosé *et al*, 2008). These results imply that kinase activity may be associated with down-regulation of the myosin motor. Results from experimentation on the kinase-removed construct have several caveats, however. It is possible that removal of the kinase domain may result in structural changes of the remaining molecule. Additionally, differentiation between effects due to autophosphorylation and those resulting from kinase-motor interactions is unclear.

To more specifically identify the role of the kinase domain in motor regulation we have expressed and purified a kinase-dead construct, myosin IIIa 2IQ K50R, in which a critical lysine in the kinase catalytic domain has been substituted with arginine to render the kinase domain incapable of autophosphorylating the motor. Cell localization studies in mouse stereocilia have been accomplished. Additionally, we have examined the concentration dependence and role of actin filaments in the autophosphorylation process of our wild-type construct, MIIIa 2IQ, and have conducted a preliminary characterization of the steady-state enzymatic activity for fully phosphorylated MIIIa 2IQ.

Previous results obtained by comparison of MIIIa 2IQ to MIIIa 2IQ ΔK suggested that autophosphorylation may down-regulate the motor by reducing its affinity for actin. Our current study provides additional support for this hypothesis as well as additional data to clarify a model for the role of myosin IIIa in sensory cells, including the ability of the kinase to phosphorylate the motor in the presence of actin filaments and the

regulation of myosin motor activity by intermolecular autophosphorylation in a concentration-dependent manner.

CHAPTER 3: MATERIALS AND METHODS

3.1. Generation of Human Myosin IIIA cDNA Constructs

Reagents used were all of the highest purity available commercially. ATP and ADP were prepared fresh from powder. Nucleotides were prepared in the presence of equimolar $MgCl_2$ before use. [γ^{32}P]ATP was purchased from GE Healthcare Biosciences or PerkinElmer Life and Analytical Sciences Inc.

We previously generated a construct of human myosin IIIa containing residues 1-1143, truncated after the second IQ domain (MIIIa 2IQ) and containing a C-terminal FLAG tag (DYKDDDDK) for purification purposes (Dosé *et al*, 2007; Sweeney, 1998; Sun *et al*, 2006). The Stratagene QuikChange site-directed mutagenesis kit (Agilent Technologies) was used to modify this construct with a single point mutation, substituting arginine for lysine at residue 50 in the catalytic site of the kinase domain (MIIIa 2IQ K50R), as described in Salles *et al* (2009). Expression plasmids were sequence verified by the University of Pennsylvania DNA Sequencing Facility.

3.2 Expression and Purification of Proteins

Recombinant baculoviruses of MIIIa 2IQ, MIIIa 2IQ K50R, and calmodulin were generated with the FastBac system (Invitrogen). MIIIa 2IQ and MIIIa 2IQ K50R, respectively, were co-expressed with calmodulin (CaM). One liter of insect Sf9 cells (2 x 10^6 cells/ml) was co-infected with myosin and CaM viruses and cultured for three days at

28°C then harvested by centrifugation. Cells were lysed in 45 ml lysis buffer (10 mM Tris pH 7.5, 200 mM KCl, 1 mM EGTA, 1 mM EDTA, 2 mM $MgCl_2$, 0.015 mg/ml aprotinin, 0.015 mg/ml leupeptin, 1 mM phenylmethylsulfonyl fluoride (PMSF), 2 mM ATP, 5 mM dithiothreitol (DTT)), and centrifuged (Beckman Coulter ultracentrifuge, Ti70 rotor) at 45 000 rpm for one hour. Myosin was separated on an anti-FLAG resin column and eluted with excess FLAG peptide. The elute was further purified by ammonium sulfate precipitation then dialyzed overnight at 4°C in KMg100 buffer (10 mM imidazole, 100 mM KCl, 1 mM EGTA, 1 mM $MgCl_2$, 1 mM DTT). Protein purity was assessed by Coomassie-stained SDS PAGE gels. The Bio-Rad microplate Bradford assay was used to determine myosin concentration, with BSA as a standard (Dosé *et al* 2006, Dosé *et al* 2008). Absorbance measurements were also performed using a predicted extinction coefficient of 129 500 $M^{-1} \cdot cm^{-1}$ to calculate the concentration, with similar results.

Actin was purified from rabbit skeletal muscle using an acetone powder method (Pardee and Spudich, 1982). Actin was extracted in cold (4^oC) G buffer (2 mM Tris-HCl pH 7.5, 0.2 mM ATP, 0.5 mM DTT, 0.2 mM $CaCl_4$, 0.01% NaN_3) and filtered, followed by polymerization at 4^oC (addition of 50 mM KCl, 2 mM $MgCl_2$, 0.8 mM ATP, and after 2 hours in high salt wash to remove tropomyosin). Following centrifugation pellets were resuspended in fresh G buffer and dialyzed for two days with buffer changes. To enhance purity a second polymerization and depolymerization cycle was completed prior to use or liquid nitrogen storage. Concentration was determined by absorbance measured at 290 nm using an ε^{290} of 2.66×10^4 M^{-1} cm^{-1}. A molar equivalent of phalloidin (Sigma) was added to stabilize actin filaments in experiments.

All experiments were performed in KMg50 buffer (50 mM KCl, 1 mM EGTA, 1mM $MgCl_2$, 1 mM DTT and 10 mM Imidazole-HCl, pH 7.0, 25^{o}C) and in the presence of excess calmodulin to ensure that the IQ domains of MIIIa had bound calmodulin.

3.3 Kinase Activity Assays

Autophosphorylation of MIIIa 2IQ and MIIIa 2IQ K50R was detected by kinase assay using [γ^{32}P]ATP. Myosin at specified concentrations was allowed to react with 200 μM [γ^{32}P]ATP at room temperature (~22^{o}C) for specific time periods ranging from 0 to 60 minutes. The reaction was stopped at each time point by the addition of SDS loading buffer. Autophosphorylation of MIIIa 2IQ K50R was compared to that of MIIIa 2IQ at 1μM concentration, as was autophosphorylation of MIIIa 2IQ in the presence of 40 μM actin. Additionally, autophosphorylation rates were compared at a series of myosin concentrations ranging from 0.1 to 1.2 μM. Samples were run on SDS-PAGE gel and the incorporation of ^{32}P into myosin IIIa was detected by phosphorimaging using the Typhoon 8600 Variable Mode Imager (Molecular Dynamics). Following phosphorimaging, the gel was Coomassie-stained to assess evenness of loading. Densitometry analysis using NIH Image J software was used to determine band intensities and adjust for loading differences.

3.4 Steady-State ATPase Activity

Steady-state ATP hydrolysis by MIIIa 2IQ K50R (50-100 nM) in the absence and presence of actin (0-60 μM) was examined by use of the nicotinamide adenine dinucleotide (NADH)-linked assay (Dosé *et al*, 2006) with a final MgATP concentration of 1mM. This assay employs the NADH–lactate dehydrogenase–pyruvate kinase–

phosphoenol pyruvate (NADH-LDH-PK-PEP) regeneration system to quantify the ATP hydrolysis rate by coupling regeneration of ATP hydrolysis product (ADP) to NADH oxidation, determined by monitoring for 200 s at an absorbance of 340 nm. The assay was performed in an Applied Photophysics stopped-flow. The ATPase rate at each actin concentration was determined, and Michaelis-Menten equation was used to calculated the k_{cat} and K_{ATPase} [V_o + ((k_{cat} [actin])/(K_{ATPase} + [actin]))]. Uncertainties are reported as standard errors in the fits unless stated otherwise. The data at each actin concentration represents an average of 2-3 protein preparations.

For comparing steady-state ATP hydrolysis rates of phosphorylated and unphosphorylated MIIIa 2IQ at 20 µM actin, we pre-incubated the myosin (1-4 µM) at room temperature for 60 minutes with either 200 µM ATP or buffer, taking samples at specific time points (5, 15, 30, 60 min). Myosin was diluted into the assay in the presence of 20 µM actin, ATP, and the regeneration system. The ATPase rate as a function of time incubated was fit to a single exponential equation.

Steady-state actin-activated ATPase rates for both phosphorylated and unphosphorylated MIIIa 2IQ were obtained by preincubation of MIIIa 2IQ for 60 min (as described above) immediately prior to the assay. Samples were tested in the presence of 0 - 60 µM actin as described above. Separate incubations were conducted for each ATPase sample using staggered start times to ensure that the lag time between incubation and testing was consistent.

3.5 Actin Co-Sedimentation Assays

Steady-state actin affinity of MIIIa 2IQ K50R as well as phosphorylated and unphosphorylated MIIIa 2IQ was determined by actin cosedimentation. The PK-PEP

ATP regeneration system was used to eliminate the accumulation of ADP. Myosin (1 μM) was mixed with actin (0-60 μM) in the presence of the regeneration system. 1-2 mM ATP was added prior to ultracentrifugation in a TLA 100.2 Beckman centrifuge at 95 000 rpm for 20 min at 25° C. Supernatant and pellet were separated, the pellet was resuspended in KMg50-DTT buffer, and samples were run on SDS-PAGE gels. The fraction of actin-bound myosin was determined by measuring the relative amount of myosin in the pellet sample normalized to the total (supernatant + pellet). Quantification of bands and densitometry analysis were performed using Image J software (NIH). Kaleidagraph software was used to fit the data to a binding equation.

CHAPTER 4: RESULTS

4.1 Kinase-Dead Mutant MIIIA 2IQ K50R

The expression yields of MIIIa 2IQ K50R co-expressed with calmodulin in the baculovirus insect cell (sf9) system were comparable to those for MIIIa 2IQ in this and our previous studies (Dosé *et al* 2006; Dosé *et al* 2008). The purity of both MIIIa 2IQ (WT) and MIIIa 2IQ K50R after anti-FLAG affinity column chromatography was assessed to be 95% by Coomassie staining following electrophoresis in SDS-PAGE gel (expected molecular weight for each construct was 131 780 Da). Stoichiometry for calmodulin to myosin was determined to be approximately two to one.

All experiments were performed in KMg50 buffer in the presence of 10-fold excess calmodulin to ensure that all IQ motifs were calmodulin-bound. Conditions and methods for experiments were identical to those in our previous kinetic characterizations of MIIIa 2IQ and MIIIa 2IQ ΔK (Dosé *et al* 2006, Dosé *et al* 2008) unless otherwise indicated, which allow direct comparison with the current kinase-dead and fully-phosphorylated myosin IIIA analyses. We investigated properties of the phosphorylation process in addition to the steady-state activity of a fully phosphorylated MIIIa 2IQ. Full phosphorylation was accomplished by incubation of myosin with 200 μM ATP in the presence of 10 μM calmodulin (at room temperature, 60 minutes) as described in Dosé *et al* (2006), then immediately used in the assay.

The elimination of kinase activity by the K50R point mutation was evaluated by Western blot of samples taken at specific time points during 60 minutes of incubation with 200 μM ATP, using antiphosphothreonine as the primary antibody (Figure 1). No phosphothreonine increase was detected at a myosin concentration of 0.5 μM, whereas the myosin IIIa 2IQ wild type protein (0.5 μM) showed similar rates of increase in phosphorylation to our previous reports (Dosé *et al*, 2006). Prior to incubation (0 min) the K50R myosin showed a residual level of threonine phosphorylation slightly higher than was previously seen and reported for the wild type control (Dosé *et al*, 2006). Nitrocellulose membranes were stripped and reprobed with anti-FLAG to evaluate evenness of protein loading for each sample.

4.2 Myosin Concentration Dependent Autophosphorylation

To determine whether autophosphorylation of myosin IIIa is an intermolecular or intramolecular process, we performed time-course kinase assays in the presence of 200 μM (γ^{32}-P) ATP as described in Materials and Methods, at a series of myosin concentrations between 0.1 μM and 1.2 μM. Phosphorimages of representative SDS-PAGE gels from one experiment are shown in Figure 2C (0.1, 0.3, 0.6 and 1.2 μM). After phosphorimaging, gels were Coomassie-stained to determine total protein levels. Densitometry analysis was used to determine the time course of phosphate incorporation at each concentration based on the phosphorylated band intensity relative to total protein levels. Results are averaged from 3-4 separate experiments on three different protein preps.

We found that autophosphorylation rates were nearly linearly dependent on myosin concentration within the range tested (Figure 2, A and B). Rates obtained were

as follows: at 0.1μM, 0.049 ± 0.035 min^{-1}; at 0.3 μM, 0.116 ± 0.029 min^{-1}; at 0.6μM, ~0.207 ± 0.064 min^{-1}; and at 1.2μM the rate was 0.289 ± 0.060 min^{-1}. The data were fit to a hyperbolic equation [kinase activity / (sec * [MIII])] → [kinase activity (relative) / (sec * [mM M3])] to estimate the maximum kinase activity rate. The dependence of phosphorylation rate on myosin concentration suggests an intermolecular process for autophosphorylation in MIIIa 2IQ.

4.3 Actin Concentration Independent Autophosphorylation

An early study predicted that the autophosphorylated residue(s) of the human myosin IIIa motor is/are within a 20-kDa segment at its C terminus, near loop 2 of the motor's actin-binding region (Komaba *et al* 2003). In order to determine whether the MIIIa motor in the presence of actin is autophosphorylatable in the same way as myosin alone, we performed parallel time-course kinase assays incubating myosin IIIa 2IQ in the absence and the presence of 40 μM actin with 200 μM (γ^{32}P)ATP. Kinase assays were performed as described in Materials and Methods, and results were visualized by SDS-PAGE and phosphorimaging, as well as Coomassie staining (Figure 3B). By densitometry analysis we determined that the presence of actin had no appreciable influence on phosphorylation rate (Figure 3A). Results are averaged from 3-4 separate experiments on three different protein preps.

4.4 Steady State ATPase Activity

We evaluated the steady-state enzymatic activity of MIIIa 2IQ K50R as compared to that of the wild-type MIIIa 2IQ construct in its phosphorylated state, using the NADH-coupled actin-activated ATPase assay as described in Materials and Methods (Figures 4A

and 4B). The unphosphorylated control MIIIa 2IQ was treated in parallel with phosphorylated samples but in the absence of ATP.

We plotted the ATPase activity as a function of actin concentration and used the Michaelis-Menten equation to determine k_{cat} and K_{ATPase}. As previously reported the maximal ATPase activity (k_{cat}) for the kinase dead construct was 0.76 ± 0.08 sec^{-1} (Salles et al 2009), while the actin concentration at one-half maximum ATPase activity, $K_{ATPase,}$ was 11.9 ± 3.7 μM (Figure 4B). The k_{cat} for the kinase dead construct is comparable to our previous results on MIIIa 2IQwt (0.77 ± 0.08 sec^{-1}), but its K_{ATPase} was 3-fold lower, intermediate between MIIIa 2IQ (34 ± 11μM) and MIIIa 2IQ ΔK (1.4 ± 0.04 μM) (Table 1) (Salles et al, 2009, Dosé *et al*, 2007, Dosé *et al*, 2008).

We evaluated the effect of phosphorylation on MIIIa 2IQ's steady-state rate of ATP hydrolysis at a constant actin concentration (Figure 4A). MIIIa 2IQ (1 μM) was incubated with 200 μM ATP at room temperature (~22^{o}C) and samples were taken at four time points during the phosphorylation process (5, 15, 30, 60 min) to be immediately run in the assay in the presence of 20 μM actin and the regeneration system. A buffer-treated control at the same concentration was assayed in parallel with each sample (Figure 4A). Results indicate that, compared to the control, enzymatic activity was reduced as myosin phosphorylation progressively increased. After 60 minutes of incubation the ATPase rate for phosphorylated MIIIA 2IQ at 20 μM actin was 0.099 ±0.057 sec^{-1}, a reduction in activity of approximately 40% relative to the control. Room temperature buffer treatment did not appreciably alter the control myosin's ATPase rate of 0.245 ± 0.067 sec^{-1}. Results are averaged from 3-4 separate experiments on three different protein preps.

We measured the steady-state actin-activated ATPase activity of fully phosphorylated MIIIA 2IQ with a range of actin concentrations (0-40 μM) and compared it to unphosphorylated controls. Our results indicate that the maximum ATPase rate (k_{cat}) was reduced by phosphorylation (0.25 ± 0.077 sec^{-1} compared to 0.78 ± 0.30 sec^{-1}) as was the K_{ATPase} (2.38 μM ± 3.38 compared to 24.9 μM ± 19.7 for unphosphorylated) (Figure 4B). Results for the controls were similar to those obtained in our previous analysis of untreated MIIIa 2IQ (Dosé *et al*, 2007).

4.5 Steady State Actin Affinity

We determined the steady-state actin affinity of myosin IIIa 2IQ K50R in the presence of ATP and the PK-PEP regeneration system using a co-sedimentation assay as described in Materials and Methods. The fraction of myosin that bound to actin was plotted as a function of actin concentration (0 – 40μM), and fit to a hyperbolic equation to determine the steady-state actin affinity (K_{Actin}) of 3.83 ± 0.53 μM. This value is intermediate between previous results obtained for the wild type MIIIa 2IQ and kinase-deleted MIIIa 2IQ ΔK (7.0 μM ± 0.6 μM and 1.4 ± 0.4 μM, respectively) (Figure 5A and B, MIIIa 2IQ K50R). Results represent the average from three separate experiments from two different protein preparations.

The actin co-sedimentation assay was also performed on fully phosphorylated MIIIa 2IQ in parallel with buffer-treated controls. Samples of phosphorylated and unphosphorylated control MIIIa 2IQ were prepared as described above (60m incubation at room temperature in the presence and absence of 200 μM ATP) and immediately run in the assay at 1 μM concentration. As seen in Figure 5, the steady-state actin affinity of phosphorylated MIIIA 2IQ was lower than the control, with a K_{Actin} (actin concentration

at one-half maximum) of 15.60 μM ± 2.43 as compared to 5.48 ± 1.16 for the control. Phosphorylation was consistently associated with reduced maximum fraction of actin-bound myosin (~0.65% vs. ~0.86%). (Figure 5B, phosphorylated and control). Results represent the average from 3-5 experiments on 2-3 different protein preparations.

CHAPTER 5: DISCUSSION

Previously our lab characterized the motor enzymatic activity using a kinase-removed construct (MIIIa 2IQΔK) and compared its enzymatic properties to those of its wild-type counterpart MIIIa 2IQ (Dosé *et al* 2006, Dosé *et al* 2008). Without the 34 kDa kinase domain the myosin IIIa motor demonstrated a 2-fold higher maximal ATPase rate and 5-fold tighter actin affinity, which suggests it behaves as an unregulated motor and therefore suggesting that phosphorylation may serve as a downregulatory mechanism. Our current study provides further insight by eliminating the potentially confounding influences associated with complete removal of the kinase domain by comparing the enzymatic activity of the recently-developed kinase-dead construct (MIIIa 2IQK50R) (Salles *et al* 2009) with those of a fully phosphorylated MIIIa 2IQ. We also report that the autophosphorylation process occurs intermolecularly and is independent of actin concentration, properties that are relevant to the regulation of myosin IIIa's function in the cell. These investigations provide, in conjunction with our earlier studies, a more direct evaluation of the properties and effects of myosin IIIa motor autophosphorylation. We also include corroborating evidence from immunolocalization studies using GFP-tagged versions of our constructs transfected into mouse stereocilia, which add important information for further clarification of the model.

The results of our kinase assays show that the rate of autophosphorylation increases with myosin concentration across the range of 0.1 μM to 1.2 μM, which

indicates that the autophosphorylation process takes place in an intermolecular manner in this concentration range. That is, myosin IIIa kinase domains phosphorylate other myosin IIIa target residues on nearby molecules rather than (or in addition to) sites within the same myosin IIIa protein. This suggests that as myosin IIIa motor activity propels individual molecules to actin bundle tips they join others accumulated in its tip compartment. As concentrations of myosin IIIa increase in the tip compartment myosin IIIa can phosphorylate other nearby myosin IIIa molecules and downregulate the ATPase activity as well as actin affinity.

Since myosin IIIa functions in actin-rich regions in the cell, we investigated the autophosphorylation process in the presence of actin. We conducted kinase assays in parallel in the presence and absence of actin filaments (40 μM concentration), and found that autophosphorylation rate and degree were not altered by actin *in vitro*. It appears that the motor's target residues for phosphorylation remain equally accessible to the kinase under either condition. Our results suggest a model in which the concentration of myosin IIIa localized to the compartment at the end of its bundled actin filament "track" is regulated by autophosphorylation in a concentration-dependent manner.

We recently developed the myosin IIIa construct MIIIa 2IQ K50R with a point mutation at the critical lysine in the catalytic region of the myosin's kinase domain to abolish ATP catalysis and thus render it non-functional as a kinase, while otherwise retaining its full sequence (Salles *et al* 2009). We showed by Western blot analysis using the antiphosphothreonine antibody that the K50R construct had relatively little increase in threonine phosphorylation under our assay conditions. The wild-type myosin IIIa demonstrated threonine phosphorylation which reached saturation over a one-hour time

course. This is in agreement with previously published phosphorimaging results showing no phosphorylation increase for K50R with the same treatment conditions using radiolabeled ATP (Salles *et al* 2009). Western blotting provides the additional information that, for both MIIIa 2IQ wild type and MIIIa 2IQ K50R, an initial level of threonine phosphorylation can be detected prior to beginning the assay. Initial wild type phosphorylation was also detected previously and was attributed to the activity of an exogenous kinase in the Sf-9 cells during the culturing process (Dosé *et al* 2006). Interestingly, Pak1 kinases have a highly conserved serine/threonine residue that requires phosphorylation for activation of kinase activity (Liu *et al* 2006, Pirruccello *et al* 2006). This serine/threonine can be readily phosphorylated by either exogenous or activated Pak1 kinases in an intermolecular fashion (Pirruccello *et al* 2006). The corresponding conserved residue in myosin IIIa is T184.

Of interest is the observation that initial phosphorylation levels are consistently high for K50R, whereas initial phosphorylation levels for the wild type construct are typically low. We have found that, in contrast to K50R, those wild-type preps that exhibited heavier initial phosphorylation also showed low activity in the steady-state ATPase. Our interpretation is that when a wild-type myosin IIIa prep shows heavy initial phosphorylation, activated kinase domains have already phosphorylated target sites on the motor and therefore we cannot use it to make comparisons between phosphorylated and dephosphorylated parameters. The kinase domain of the K50R construct has been rendered unable to phosphorylate either kinase or motor target residues, so it is likely that the K50R kinase activation site and/or another kinase domain phosphorylation target is

more readily accessible to an exogenous kinase and becomes phosphorylated under culture conditions, while the motor remains unphosphorylated.

Because a major goal was to investigate the effects of phosphorylation on the MIIIa motor, we evaluated the steady state enzymatic and actin binding activity of the K50R construct as representative of an unphosphorylated motor that will not become phosphorylated during an ATP-containing assay. This provided a point of reference for comparison with the steady-state activity of a fully phosphorylated myosin IIIa motor. In the ATPase assay we found the kinase-dead construct to differ from both phosphorylated and untreated/buffer-treated wild type MIIIa 2IQ in its actin-binding properties (K_{ATPase} and K_{Actin}) while the maximum rate of actin-activated enzymatic activity (k_{cat}) was unchanged between K50R and untreated wild type but reduced for phosphorylated MIIIa 2IQ. In the actin cosedimentation assay reported herein we found a K_{Actin} that was approximately 2-fold tighter than wild type (3.83 µM vs 7.0 µM), while the fully phosphorylated myosin had a higher K_{Actin} than either of these (See Table 1).

The pretreatment for full phosphorylation reduced the k_{cat} of the ATPase assay from its wild type value while the previously-reported kinase deletion increased it, yet the K50R point mutation did not cause a difference from untreated wild-type values. We attributed the enhanced maximum ATPase activity of the ΔK construct to a faster transition between two actomyosin-ADP states, which is the rate limiting step for wild type myosin IIIa (Dosé *et al* 2006, Dosé *et al* 2008). The MIIIaΔK construct has shifted its rate limiting step to ATP hydrolysis. Phosphorylation, on the other hand, may slow the transition from the intermediate to the high affinity AM.ADP state, or alternatively it may cause a large increase in the population of myosin inhabiting a previously observed off-

pathway low affinity M.ADP state (Dosé *et al* 2008, Dosé *et al* 2006). An increase in the population of the off-pathway AM.ADP state could reduce the overall k_{cat} because the rate of ADP release for this state may be slowed. It is likely, given the slow rate of autophosphorylation at the assay's myosin concentrations (~.05 min^{-1} at 0.1 µM), that not enough autophosphorylation can take place during the 200-second timecourse of the ATPase assay to effect a measurable change in $k_{cat,}$ and so only a small difference is noted between untreated/buffer-treated wild type and K50R.

In our timecourse ATPase assays we monitored the changes in steady-state ATPase rate at 20 µM actin as the time of pre-incubation with ATP increased. We found a progressive reduction to approximately 40% of the initial rate after one hour of incubation, which agrees in principle with the results from the full-range ATPase assays using fully phosphorylated myosin. However, our results from the full assay show little if any difference at 20 µM actin. One difference between the two assays was in the myosin concentration during pre-treatment (1 µM for the timecourse, 4 µM for the full-range assay). The change in pretreatment conditions improved the preservation of myosin ATPase activity for both experimental and control samples, correcting an inconsistency experienced with this assay. It is difficult to ascertain how this change might result in the difference noted, but the high-concentration pretreatment may have resulted in more thorough phosphorylation. Another possible explanation is that, during the time the full-range assays were being conducted, our preps tended to show more initial phosphorylation than the earlier preps used for the timecourse assays. As noted earlier, higher initial phosphorylation tended to correlate with lower activity in the ATPase in the

untreated and buffer-treated state, and so the assay required higher actin concentrations to distinguish the effects caused by additional phosphorylation.

Both ATPase and actin cosedimentation steady-state assays showed the K50R actin affinity to be intermediate between wild type and the previously reported high affinity seen for the kinase deleted construct (Dosé *et al* 2008), while the fully phosphorylated MIIIa sample exhibited reduced K_{ATPase} and increased $K_{Actin.}$. While both these measurements are used to describe steady-state actin affinity, they are obtained in different ways. Both employ ATP regeneration systems to minimize the buildup of ADP during the assay, which has the potential to compete with ATP at the motor's nucleotide binding site, but the time period during which the regeneration system must work is very different. If phosphorylation influences the rate of transition between AM.ADP states, then the presence of additional ADP in the system may affect phosphorylated MIIIa differently than unphosphorylated. The ATPase assay is monitored as it progresses over 200 seconds after a brief time during which reagents are mixed and loaded into the stopped-flow. On the other hand, the actin cosedimentation assay takes slightly longer to mix and load into the centrifuge, while the centrifugation step takes 20 minutes. Thus there is a greater likelihood of ADP buildup during the cosedimentation assay in spite of the regeneration system. If, as described, motor phosphorylation causes a shift in equilibrium so that the transition from the intermediate affinity AM.ADP state to the off-pathway low affinity AM.ADP state becomes more favored and the transition to the high affinity state is either slowed or not appreciably affected, the presence of ADP may be inhibitory for one or both of these transitions. The different balance in populations of the three AM.ADP states due to the presence of excess ADP would be reflected in an overall

K_{Actin} for phosphorylated MIIIa 2IQ that is higher than that seen in the unphosphorylated MIIIa 2IQ.

In collaboration with this work, the Kachar lab (NIH) has completed an analysis of full length GFP-tagged myosin IIIa K50R, ΔK and wild type transfected into mouse stereocilia, and those results will be published in conjunction with our data described herein. This is a follow-up to their immunolocalization studies in which they transfected GFP-tagged full length versions of our myosin IIIa constructs into COS-7 cells (Salles *et al*., 2009) so that their localization characteristics in an endogenous environment could be investigated (See Appendix, Supplemental Figure 1). As was seen in filopodia of COS-7 cells, myosin IIIa localized primarily to the tips of actin bundles in stereocilia, with more pronounced localization seen for the K50R construct and especially so for ΔK, both of which appear to expand the tip compartment compared to stereocilia transfected with wild type. Differences in the actin treadmilling rate of stereocilia, where treadmilling is slow, and filopodia, where treadmilling is more rapid, are expected to affect net velocity of myosin IIIa toward the tips and thus account for the more efficient wild-type myosin IIIa tip localization in stereocilia (Salles *et al* 2009). The longer stereocilia in the grouping on a given hair cell appear to have a higher concentration of myosin IIIa than the shorter ones seen in transfected wild type and K50R cells. The ΔK-transfected stereocilia in this image appear to all have high concentrations of myosin and are all of similar length rather than exhibiting the characteristic staircasing seen for transfections of the other myosin IIIa constructs. The observed relationship between myosin IIIa concentration and stereocilia length is logical for a myosin whose cellular role involves

maintenance of the length of actin bundles in structures that must maintain a precise length for function..

Our results suggest that the ability to autophosphorylate its motor is important for myosin IIIa down regulation, potentially in conjunction with maintaining the appropriate concentration of its cargo, the actin-bundling protein espin I. The combination of myosin IIIa motor regulation and espin I actin-bundling function may serve to maintain the actin bundle core at the required stereocilia length for a hair cell's auditory mechanotransduction response. Salles *et al* (2009) suggest that, rather than dissociating from one another, the myosin IIIa-espin 1 complex may be assimilated into and maintained within the actin bundle core as a unit so that the entire complex is carried to the stereocilia base by the actin treadmilling process.

It may be further speculated that in addition to espin 1 transport myosin IIIa performs other as yet undetermined role(s) when localized to stereocilia tips, which are also the site of mechanoelectrical transduction (MET). It was demonstrated that maturation of MET is developmentally correlated with onset of myosin IIIa expression above detectable levels (Waguespack *et al*, 2007), and it is suggested that myosin IIIa may be able to bind other membrane proteins with ankyrin repeats similar to those on the espin 1 WH2 domain (Salles *et al* 2009). The lack of down regulation associated with the non-functional kinase constructs has the potential to contribute to excessive lengthening of actin bundles by several means.

Phosphorylation is utilized as a regulatory mechanism for the activity of many members of the myosin superfamily. Not only is regulatory light chain phosphorylation necessary to activate the smooth muscle and non-muscle myosin II ATPase, but there are

also many examples of regulation by heavy chain phosphorylation. Non-muscle myosin II phosphorylation near the C-terminus of its tail region appears to down-regulate its activity by inhibiting filament formation and/or directly influencing its actomyosin ATPase. Tail phosphorylation appears to similarly influence activity of some unconventional myosins by affecting tail binding characteristics (Brzeska and Korn 1996 review). Some lower eukaryotic myosin I isoforms are activated by motor phosphorylation targeting a specific serine or threonine residue in an actin-binding surface loop (the TEDS site). Interestingly a Pak1-like myosin heavy chain kinase whose catalytic region is similar to the myosin IIIa kinase domain phosphorylates the TEDS site (Bement and Mooseker 1995, Brzeska and Korn 1996 review, Redowicz 2001 review). Actin-activated kinetics of the myosin VI motor are likewise modulated by phosphorylation by a cellular Pak kinase at a threonine residue in its TEDS site (De La Cruz *et al* 2001). However, the myosin IIIa motor phosphorylation does not appear to be at the TEDS residue since there is a glutamic acid at this site in myosin IIIa (Bement and Mooseker 1995; De La Cruz *et al* 2001; Dosé *et al* 2003).

The C-terminal portion of the myosin IIIa motor domain identified as its autophosphorylatable region (Komaba *et al* 2003) contains loop 2, which is a surface loop in the actin-binding region that is thought to alter actin affinity and actin-activated product release in myosin II and myosin V (Uyeda *et al* 1994, Joel *et al* 2003, Yengo and Sweeney 2004). The net positive charge in this loop appears to be a determining factor mediating actin affinity, and so the reduction in charge resulting from phosphorylation may be expected to reduce actin affinity (Joel *et al* 2003, Yengo and Sweeney 2004, Kempler *et al* 2007). It has recently been reported that *Limulus* myosin IIIa (Lp-MYO3),

an invertebrate myosin responsive to circadian rhythms but without functional motor activity, has two autophosphorylatable serines within its loop 2 region (Cardasis *et al* 2007, Kempler *et al*., 2007). Loop 2 phosphorylation has not been demonstrated for any other class of myosin, but variability in the loop's sequence and flexibility among members of the myosin superfamily is a well-documented contributor to myosin motor diversity (Uyeda *et al* 1994, Joel *et al* 2003, Yengo and Sweeney 2004).

The presence of actin did not alter autophosphorylation in spite of the possible target residue's position on or near loop 2 of the motor's actin binding region. It may be that the target residue is not in direct contact with the actin filament, and so transfer of the relatively small phosphate group is not blocked sterically. Alternatively, phosphorylation may occur in the weak binding states when myosin IIIa is detached from actin.

In summary, our results provide strong support for the hypothesis that autophosphorylation of the myosin IIIa motor domain serves to reduce steady-state actin affinity as a means of downregulating motor activity. Our kinase-dead, and thus presumably unregulated, K50R mutant demonstrated enhancement of *in vitro* steady-state actin affinity (lowered K_{ATPase} and K_{Actin}) in the actin-activated ATPase and actin cosedimentation assays. In contrast, the fully phosphorylated MIIIa 2IQ construct exhibited relatively reduced k_{cat} and increased K_{Actin} in the steady-state *in vitro* assays, along with progressive reduction in steady-state ATPase activity at a constant actin concentration as phosphorylation levels increase over time.

Our model of myosin IIIa functionality in inner ear hair cells, which is diagrammed in figure 6, proposes that the unphosphorylated myosin molecule translocates to actin bundle tips carrying espin I as its cargo. Upon arrival its kinase

domain may phosphorylate other myosin IIIa molecules in its vicinity at the tips, a process whose likelihood increases with myosin IIIa (and thus espin I) concentration. Inactivation of the myosin motor and/or reduction in actin affinity will result in detachment from the actin bundle and subsequent removal from the area by either diffusion or by actin treadmilling due to maintenance of espin 1 binding or if the actin-binding tail domain remains attached to recycling actin monomers. A possible consequence of rapid phosphorylation at high myosin concentrations may be that the espin I cannot become incorporated into actin bundle tips before myosin motor phosphorylation and inactivation causes it to be removed from the vicinity. This scenario provides a possible mechanism for myosin IIIa/espin I maintenance of stereocilia length in inner ear hair cells. It is also possible that myosin IIIa, espin I, or the myosin IIIa-espin I complex may interact at stereocilia tips with components of the MET machinery (Salles *et al* 2009).

The biological events modeled for myosin IIIa activity require a regulation strategy not only for phosphorylation via the myosin IIIa kinase domain but also for its dephosphorylation. However, the cellular phosphatase responsible for dephosphorylating the target serine/threonine residues on myosin IIIa motor and kinase domains *in vivo* has not yet been identified, and future studies on the dephosphorylation processes involved will be required for clarification. The bulk of serine-threonine dephosphorylations are catalyzed by a handful of phosphatase catalytic subunits that, in the absence of their regulatory subunits, appear to be promiscuous and unregulated enzymes (Gallego and Virshup, 2005; Virshup and Shenolikar, 2009). *In vivo*, however, these subunits combine so that the diverse regulatory components confer selectivity, localization, and regulation

to the individual phosphatase (Gallego and Virshup, 2005; Virshup and Shenolikar, 2009). Previously we have successfully dephosphorylated purified myosin IIIa using catalytic subunits of both calf intestinal phosphatase (CIP) and protein phosphatase type 1 (PP1) (data not shown). Determination of specific targeting subunits of serine/threonine phosphatases involved and their localization in stereocilia will be important to building an understanding of the reversibility of this signaling pathway (Ceulemans and Bollen, 2004; Gallego and Virshup, 2005).

Further characterization of human myosin IIIa motor regulation by autophosphorylation will also include phosphorylation site determination and direct investigation of the regulatory properties of each site by mutagenesis. In addition, a complete kinetic characterization of the phosphorylated myosin IIIa enzymatic cycle will ascertain its specific steps that are directly affected by autophosphorylation. Finally, *in vitro* motility assays of full-length myosin IIIa, both phosphorylated and unphosphorylated, will provide important data concerning its motility on actin filaments in either state. These characterizations will provide further clarification of the mechanism(s) whereby myosin IIIa contributes to the hearing process. Such studies may also have further implications regarding the proposed role for myosin IIIa in morphogenesis and maintenance of actin bundles at vertebrate photoreceptors (Lin-Jones *et al* 2004). Comparison of the two isoforms, myosin IIIa and myosin IIIb, will be critical for understanding the role of myosin III in sensory cells.

The broad goals for understanding myosin IIIa function and regulation are to develop a more complete picture of the auditory and visual sensory processes, which will provide a basis upon which treatments for hearing or visual disorders may be developed.

For example, regulation of myosin IIIa kinase activity may be critical when specific signaling pathways in which myosin III is involved become elucidated. Therapies targeting specific steps in kinase-dependent signaling pathways have been well utilized in the drug development industry. Finally, understanding the regulation of the motor and kinase activity of myosin III will allow us to develop the necessary tools to dissect its role in the sensory transduction process *in vivo.*

CHAPTER 6: SUMMARY AND CONCLUSIONS

This dissertation reports our findings on the steady-state enzymatic characteristics and actin-binding properties of both fully-autophosphorylated and kinase-dead myosin IIIa 2IQ. It also shows that the autophosphorylation process is intermolecular, as evidenced by a rate that is dependent on the myosin concentration, and that it takes place at the same rate whether actin filaments are present or not. We present a model of myosin IIIa activity in the stereocilia of inner ear hair cells that describes concentration-dependent downregulation of the myosin IIIa motor by autophosphorylation as a vital component of its role in parallel actin bundles such as those in stereocilia. Finally, we suggested lines of further investigation that are necessary to clarify specific aspects of myosin IIIa regulation as it contributes to maintenance of stereocilia structure in the hearing process.

In addition to the results presented in these chapters, the Appendix that follows includes data collected and analyzed for previously published work and results from unpublished experiments that furthered our understanding of myosin IIIa autoregulation and gave focus to the dissertation.

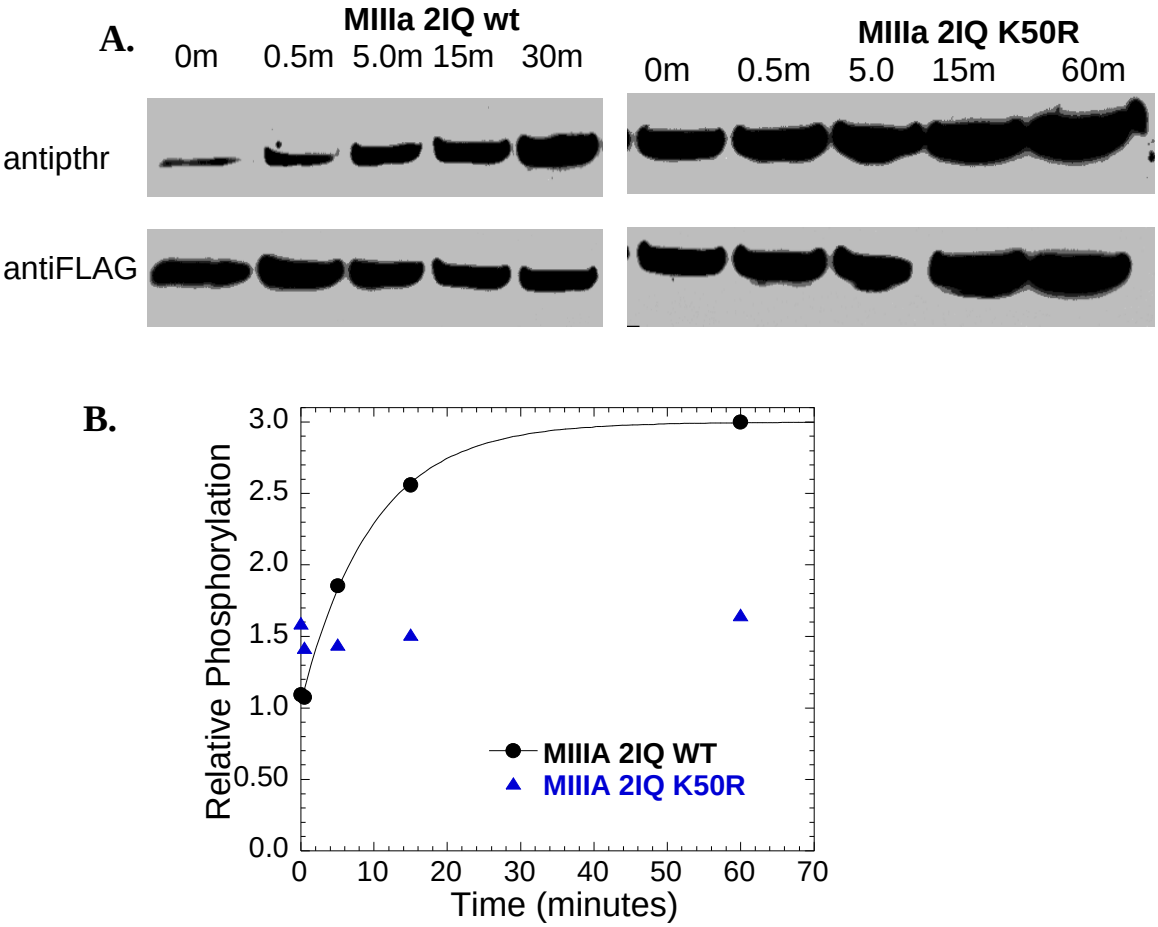

Figure 1. The myosin IIIa kinase domain was inactivated by the K50R mutation. A. The K50R mutation abolished autophosphorylation in the MIIIa 2IQ K50R mutant as compared to full phosphorylation of the wild type construct in the time course kinase assay (1.0 µM MIIIa, 200 µM ATP, 20° C) as evidenced by Western blotting, using antiphosphothreonine as the primary antibody. Stripping and reprobing with antiflag reveal relative protein levels per lane. B. Densitometry analyis of Western results. The observed high initial levels of threonine phosphorylation have been attributed to kinase phosphorylation in cell culture (See Discussion). Previously-published phosphorimaging results for K50R showed no incorporation of ^{32}P from (γ-^{32}P)ATP incubation as compared to wild type MIIIa 2IQ (Salles *et al* 2009).

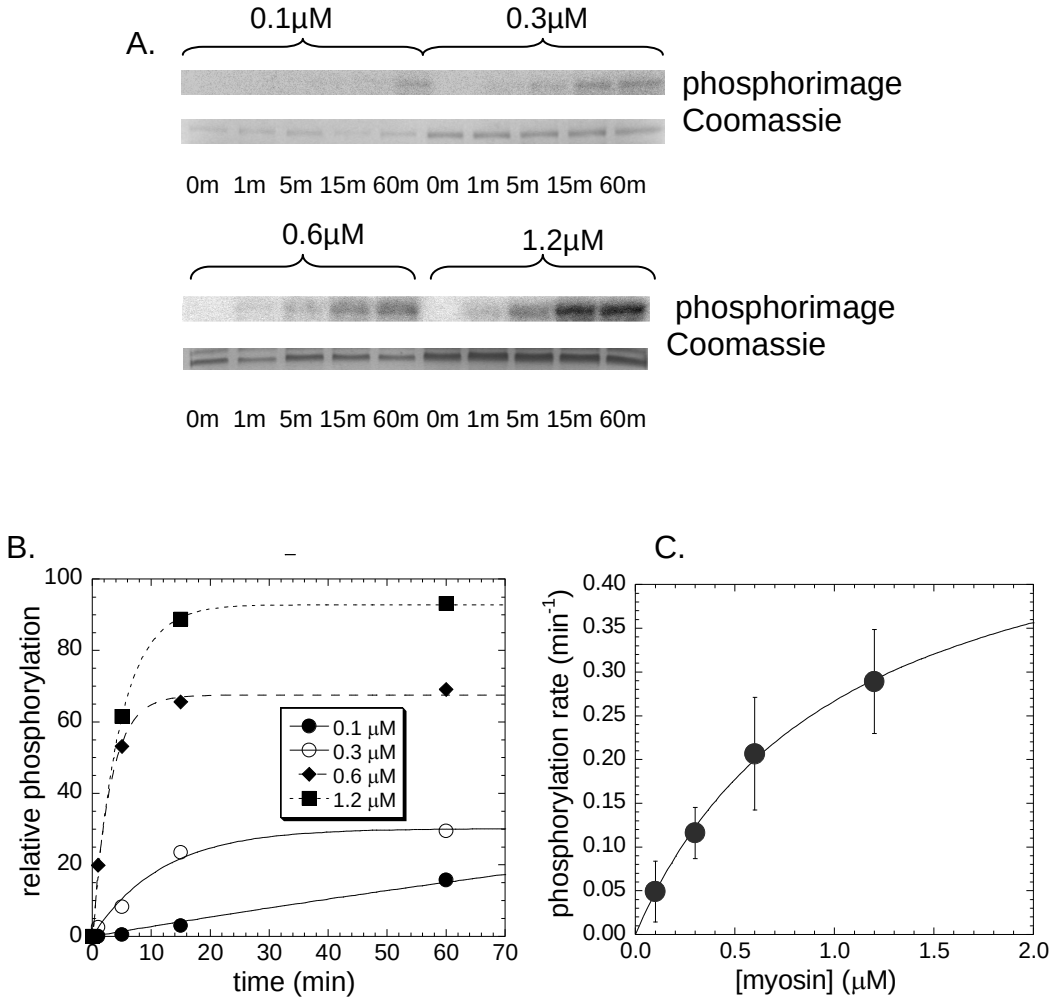

Figure 2. Autophosphorylation rates were found to be dependent upon myosin concentration. Myosin concentration dependence suggests that autophosphorylation is an intermolecular event across the range of 0.1- 1.2 µM myosin IIIa 2IQ, treated with 200µM (γ^{32}-P)ATP. A. Phosphorimages of representative phosphorylation time courses at 0.1, 0.3, 0.6, 1.2 µM myosin IIIa 2IQ, and B. densitometry analysis of a representative experiment. C. The rate of autophosphorylation ranged from 0.049 min^{-1} at 0.1 µM MIIIa to 0.289 min^{-1} at 1.2 µM MIIIa, with a V_{max} of 0.537 ± 0.047 (Error bars indicate standard deviation from 3-4 assays on 2-3 different protein preps.)

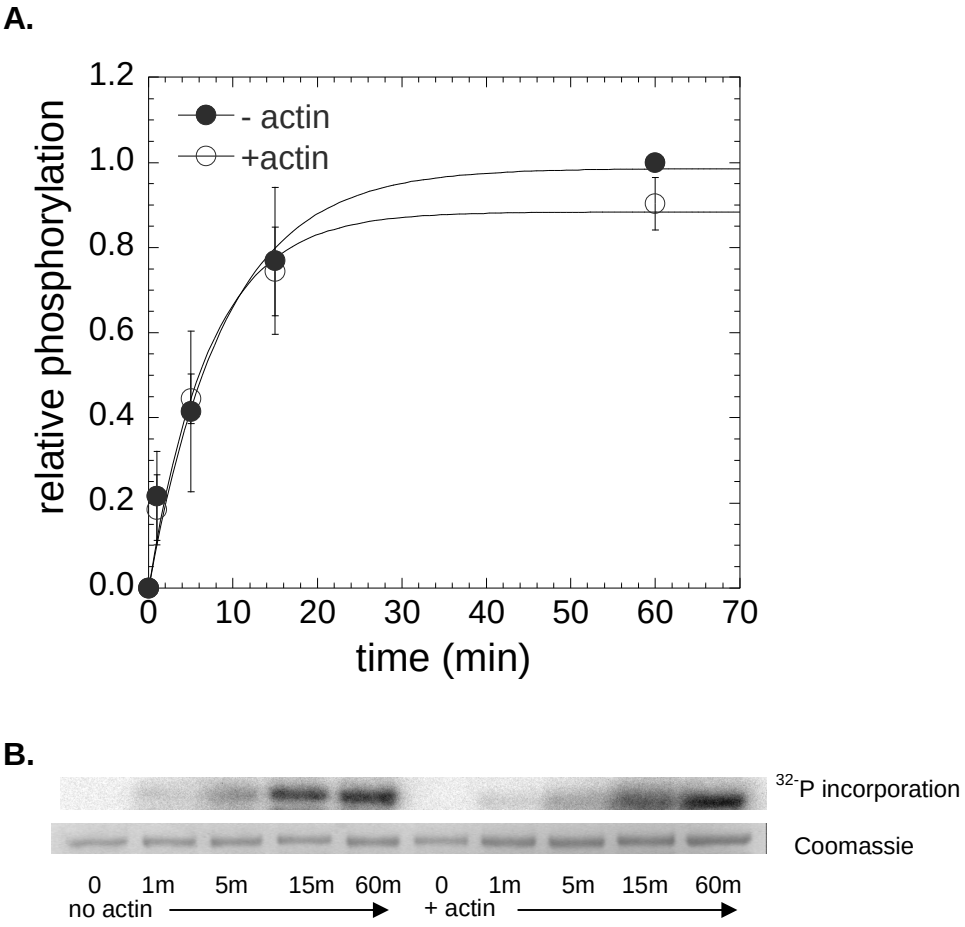

Figure 3. The presence of actin does not alter the rate of myosin IIIa autophosphorylation. A. The rate of autophosphorylation (γ-^{32}P incorporation) by 1 μM MIIIa 2IQ was unchanged in presence of 40 μM actin. ($0.0018 \pm 0.004\ s^{-1}$ vs $0.0023 \pm .0004\ s^{-1}$) Error bars represent standard deviation from 5-6 different assays using protein from several different preps. B. Representative timecourse of γ-^{32}P incorporation (0-60 m) in the presence and the absence of actin (phosphorimage). Coomassie staining indicates relative levels of total protein.

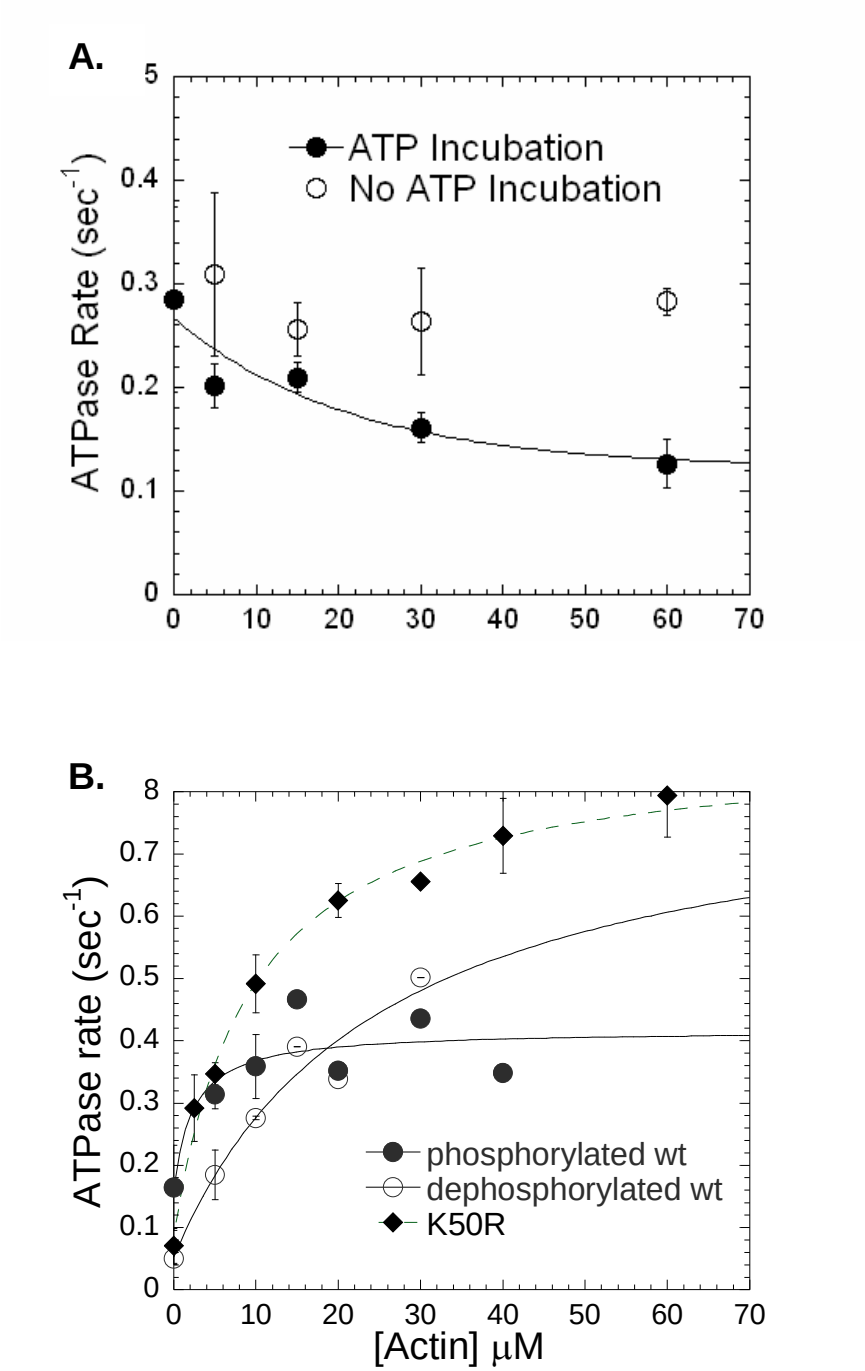

Figure 4. Steady-state actin-activated ATPase parameters for MIIIa 2IQ are influenced by phosphorylation status and by a non-functional kinase. A. As autophosphorylation progresses over time (0-60 min) the actin-activated ATPase rate (20 µM actin) decreases. Pretreatment of myosin (1 µM) was conducted as described, then diluted to 0.1 µM for the assay. B. While phosphorylation of MIIIA 2IQ reduces k_{cat} and K_{ATPase} in the actin-activated ATPase assay, the K50R kinase dead mutation reduces K_{ATPase} without changing k_{cat} from untreated MIIIa 2IQ values. Myosin concentration for pretreatment was 4 µM, and was diluted to 0.1 µM for the assay. (See Table 1 and Materials and Methods).

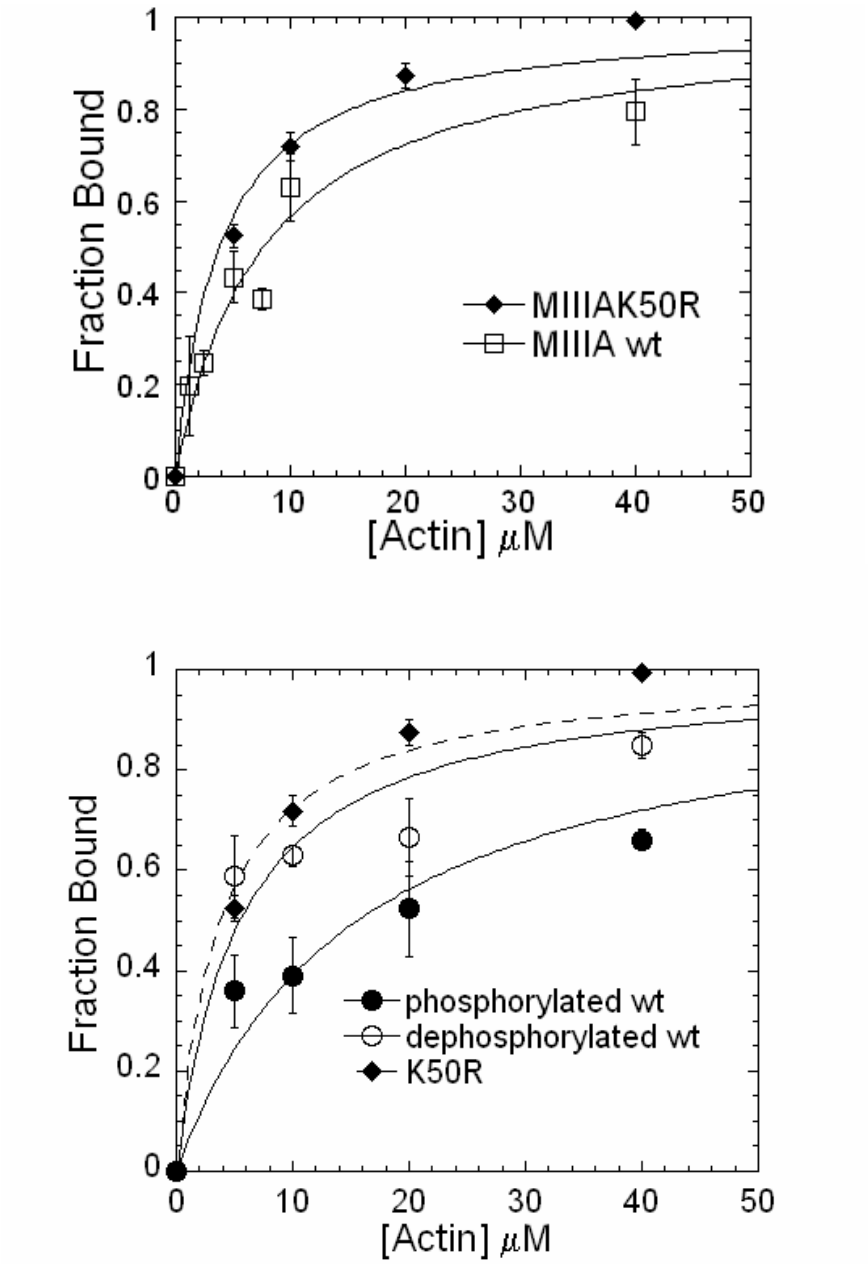

Figure 5. The steady-state affinity of MIIIa 2IQ K50R for F-actin in the presence of ATP as compared to untreated and phosphorylated MIIIa 2IQ. The actin cosedimentation assay was used to determine steady state actin affinity for (A) K50R vs untreated and (B) K50R vs phosphorylated and buffer-treated control wild type. Myosin (1.0 μM) was equilibrated in the presence of various concentrations of actin, ATP, and the ATP-regeneration system and then pelleted at 25 °C. The fraction of myosin bound to actin was quantified by densitometry analysis following Coomassie staining of SDS-PAGE gels. The plot of the fraction bound as a function of actin concentration was fit to a hyperbola to determine the steady-state affinity for actin. Error bars represent the standard deviation from 3-5 separate experiments performed on 2-3 different protein preparations. See Table 1 for values.

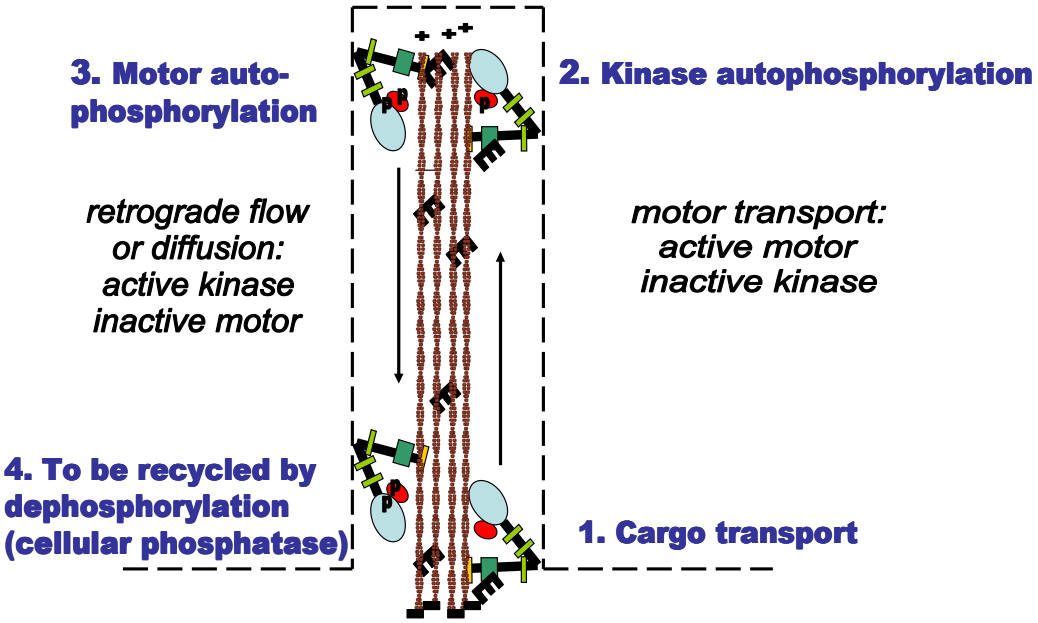

Figure 6. Model of myosin IIIa function in inner ear hair cells. 1. (*lower right*) Myosin IIIa with its cargo, espin 1, attached to its 3THD1 domain, walks up the actin bundle by motor activity and using the actin binding motif in its tail tip 3THDII domain to maintain processivity. 2. (*upper right*) Myosin IIIa may or may not release espin 1 at the tip of the actin bundle, Tail domains with or without espin 1 may remain attached to actin or, alternatively, bind with other binding partners at the tail tip. 3. (*upper left*) A cellular kinase (or another activated myosin IIIa kinase) phosphorylates the kinase domain to activate it, and it may act as a signaling protein to phosphorylate other target molecules. Other activated myosin IIIa kinases in the vicinity phosphorylate the myosin IIIa motor, reducing its actin affinity. 4. (*lower left*) Fully phosphorylated myosin IIIa returns to the base of the stereocilium by retrograde flow as it maintains association with the actin bundle. Alternatively, it may detach from the actin bundle and diffuse away from it. 5. The kinase and the motor are dephosphorylated by a cellular phosphatase.

Steady-State Parameters	MIIIa 2IQ Untreated	MIIIa 2IQ K50R	MIIIa 2IQ Phos	MIIIa 2IQ Dephos
[a]V_0 (sec)-1	0.07 ± 0.03	0.07 ± 0.05	0.16 ± 0.06	0.05 ± 0.04
[b]k_{cat} (sec)-1	0.77 ± 0.08	0.76 ± 0.08	0.25 ± 0.08	0.78 ± 0.30
[c]K_{ATPase} (μM)	34 ± 11	9.42 ± 1.68	2.38 ± 3.40	25.0 ± 19.7
[d]K_{Actin} (μM)	7.0 ± 0.60	3.83 ± 0.53	15.60 ± 2.31	5.48 ± 1.16

[a]Steady-state ATPase activity in the absence of actin measured with the NADH coupled assay.
[b]Maximum rate of actin-activated ATPase measured with the NADH coupled assay. The values for K_{ATPase} and k_{cat} were determined from the fit of the data in Figure 2 to the equation: (V_0 + (k_{cat} [actin]) / (K_{ATPase} + [actin])).
[c]Actin concentration at which the actin-activated ATPase rate is one-half maximal from the NADH assay.
[d]Actin concentration at which the myosin bound to actin in the actin cosedimentation assay is one-half of the total myosin in the assay.

Table 1. Steady-state parameters: MIIIA K50R vs. MIIIA wt untreated and after 60 min incubation with or without ATP. The kinase-inactivating mutation alters the K_{ATPase} but does not affect V_0 or k_{cat} for the steady-state ATPase cycle as compared to untreated wild type. Prior phosphorylation as described in Materials and Methods resulted in reduced k_{cat}, increased V_o, and increased K_{Actin} for MIIIa 2IQ wt, while incubation in the absence of ATP (dephos) did not appreciably alter steady state parameters from the untreated values.

REFERENCES

Alberts B, Johnson A, Lewis J, Raff M, Roberts K, Walter P. (2002). *Molecular Biology of the Cell,* 4th edition. Garland Science, Taylor and Francis Group: New York NY.

Bement WM and Mooseker MS. (1995). TEDS rule: a molecular rationale for differential regulation of myosins by phosphorylation of the heavy chain head. *Cell Motil Cytoskeleton.* 31(2):87-92.

Brzeska H and Korn ED. (1996). Regulation of class I and class II myosins by heavy chain phosphorylation. *J Biol Chem.* 271(29): 16983-16986. (Review).

Buss F and Kendrick-Jones J. (2008). How are the cellular functions of myosin VI regulated within the cell? *Biochem Biophys Res Commun*. 369(1): 165-175. (Review)

Ceulemans H and Bollen M. (2004). Functional diversity of protein phosphatase 1, a cellular economizaer and reset button. *Physiol Rev*. 84: 1-39.

Cheney RE, Riley MA, and Mooseker MS. (1993). Phylogenetic analysis of the myosin superfamily. *Cell Motil. Cytoskeleton* 24: 215–223.

Daniels RH and Bokoch GM. (1999). p21-activated protein kinase: a crucial component of morphological signaling? *Trends Biochem Sci*. 24(9):350-5. Review.

De La Cruz EM and Ostap EM. (2004). Relating biochemistry and function in the myosin superfamily. *Curr Opin Cell Biol* 16(1):61-7.

De La Cruz EM, Ostap EM, Sweeney HL. (2001). Kinetic mechanism and regulation of myosin VI. *J Biol Chem.* 276: 32373-32381.

Dosé AC and Burnside B. (2000). Cloning and chromosomal localization of a human class III myosin. *Genomics*. 67: 333-342.

Dosé AC, Ananthanarayanan S, Moore JE, Burnside B, Yengo CM. (2006). Kinetic mechanism of myosin IIIa. *J Biol Chem*. 282: 216-231.

Dosé AC, Hillman DW, Wong C, Sohlberg L, Lin-Jones J, Burnside B. (2003). Myo 3A, One of two class III myosin genes expressed in vertebrate retina, is localized to calycal processes of rod and cone photoreceptors and is expressed in the sacculus. *Mol Biol Cell.* 14: 1058-1073.

Dosé AC, Ananthanarayanan S, Moore JE, Corsa AC, Burnside B, Yengo CM. (2008). The kinase domain alters the kinetic properties of the myosin IIIa motor. *Biochemistry*. 47: 2485-2496.

Foth BJ, Goedecke MC, Soldati D. (2006). New insights into myosin evolution and classification. *Proc Natl Acad Sci USA.* 103: 3681-3686.

Friedman LM, Dror AA, Avraham KB. (2007). Mouse models to study inner ear development and hereditary hearing loss. *Ins J Dev Biol*. 51: 609-631.

Gallego M and Virshup DM. (2005). Protein serine/threonine phosphatases: life, death, and sleeping. *Curr Op Cell Biol.* 17(2): 197-202.

Harcrave PA and McDowell JH. (1992). Rhodopsin and phototransduction: a model system for G protein-linked receptors. *FASEB J.* 6:2323-2331.

Hemmer W, McGlone M, Tsigelny I, and Taylor SS. (1997). Role of the glycine triad in the ATP-binding site of cAMP-dependent protein kinase**.** *J Biol Chem.* 272: 16946-16954.

Hirai TJ, Tsigelny I, Adams JA. (2000). Catalytic assessment of the glycine-rich loop of the v-Fps oncoprotein using site-directed mutagenesis**.** *Biochemistry* 39 (43): 13276-13284

Huxley HE. (1971). Structural changes during muscle contraction. *Biochem J*. 125 (4): 85P.

Ikenoue T, Hikiba Y, Kanai F, Aragaki J, Tanaka Y, Imamura J, Imamura T, Ohta M, Ijichi H, Tateishi K, Kawakami T, Matsumura M, Kawabe T and Omata M. (2004)**.** Different effects of point mutations within the *B-Raf* glycine-rich loop in colorectal tumors on mitogen-activated protein/extracellular signal-regulated kinase kinase and nuclear factor κB pathway and cellular transformation. *Cancer Research* 64, 3428-3435.

Joel PB, Sweeney HL, Trybus KM. (2003). Addition of lysines to the 50/20 KDa junction of myosin strengthens weak binding to actin without affecting the maximum ATPase activity. *Biochemistry*. 42: 9160-9166.

Katti C, Dalal JS, Dosé AC, Burnside B, Battelle BA. (2009). Cloning and distribution of myosin 3B in the mouse retina: Differential distribution in cone outer segments. *Exp Eye Res.* 89: 224-237.

Kempler K, Toth J, Yamashita R, Mapel G, Robinson K,, Cardasis H, Stevens S, Sellers JR, and Battelle BA. (2007). Loop 2 of *Limulus* myosin III is phosphorylated by protein kinase A and autophosphorylation. *Biochemistry.* 46, 4280-4293.

Komaba S, Inoue A, Maruta S, Hosoya H, Ikebe M. (2003). Determination of human myosin III as a motor protein having a protein kinase activity. *J. Biol. Chem.* 278 (24): 21352-21360.

Krementsov DN, Krementsova EB, and Trybus KM. (2004). Myosin V: regulation by calcium, calmodulin, and the tail domain. *J Cell Biol*. 164(6): 877-885.

Lei M, Lu W, Meng W, Parrini MC, Eck MJ, Mayer BJ, and Harrison SC. (2000). Structure of PAK1 in an autoinhibited conformation reveals a multistage activation switch. *Cell* 102: 387–397.

Lei M, Robinson MA, and Harrison SC. (2005). The active conformation of the PAK1 kinase domain. *Structure*. 13: 769–778 (review).

Lin-Jones J, Sohlberg L, Dosé AC, Breckler J, Hillman DW, Burnside B. (2009). Identification and localization of myosin superfamily members in fish retina and retinal pigmented epithelium. *J Comp Neurol.* 513: 209-223.

Liu CH, Satoh AK, Postma M, Huang J, Ready DF, Hardie RC. (2008). Ca2+-dependent metarhodopsin inactivation mediated by calmodulin and NINAC myosin III. *Neuron.* 59(5):778-789.

Lu H, Krementsova EB, Trybus KM. (2006). Regulation of myosin V processivity by calcium at the single molecule level. *J Biol Chem.* 281(42): 31987-31994.

Matsumoto H, Isono I, Pye Q, Pak WL. (1987). Gene encoding cytoskeletal proteins in *Drosophila* rhabdomeres. *Proc Natl Acad Sci USA.* 84: 985-989.

Montell C and Rubin GM. (1988). The Drosophila ninaC locus encodes two photoreceptor cell specific proteins with domains homologous to protein kinases and the myosin heavy chain head. *Cell* 52: 757-772.

Morris CA, Wells AL, Yang A, Chen LQ, Baldacchino CV, Sweeney HL. (2003). Calcium functionally uncouples the heads of myosin VI. *J Biol Chem*. 278: 23324-23330.

Murphy CT and Spudich JA (1999). The sequence of the myosin 50-20K loop affects myosin's affinity for actin throughout the actin-myosin ATPase cycle and its maximum ATPase activity. *Biochemistry* 38: 3785-3792.

Ng KP, Kambara T, Matsuura M, Burke M, and Ikebe M. (1996). Identification of myosin III as a protein kinase. *Biochem.* 35: 9392-9399.

Odronitz F and Kollmar M. (2007). Drawing the tree of eukaryotic life based on the analysis of 2,269 manually annotated myosins from 328 species. *Genome Biol.* 8(9): R196.

Olivares AO, Chang W, Mooseker MS, Hackney DD, and De La Cruz EM. (2006). The tail domain of myosin Va modulates actin binding to one head. *J Biol Chem*. 281(42): 31326-31336.

Parrini MC, Lei M, Harrison SC, Mayer BJ. (2002). Pak1 kinase homodimers are autoinhibited in *trans* and dissociated upon activation by Cdc42 and Rac1. *Molec Cell*. 9: 73-83.

Petit C, Levilliers J, Hardelin JP. (2001). Usher syndrome: from genetics to pathogenesis. *Annu Rev Genet.* 35: 589 – 646.

Pirruccello M, Sondermann H, Pelton JG, Pellicena P, Hoelz A, Chernoff J, Wemmer DE, Kuriyan J. (2006). A dimeric kinase assembly underlying autophosphorylation in the p21 activated kinases. *J Mol Biol.* 361: 312-328.

Redowicz MJ. (2001). Regulation of nonmuscle myosins by heavy chain phosphorylation. *J Musc Res Cell Mot*. 22: 163-173.

Redowicz MJ. (2002). Myosins and patology: genetics and biology. *Acta Biochim Pol.* 49(4): 789-804.

Rennefahrt UEE, Deacon SW, Parker SA, Devarajan K, Beeser A, Chernoff J, Knapp S, Turk BE, and Peterson JR. (2007). Specificity profiling of Pak kinases allows identification of novel phosphorylation sites. *J Biol Chem.* 282 (21): 15667 – 15678.

Richards TA and Cavalier-Smith T. (2005). Myosin domain evolution and the primary divergence of eukaryotes. *Nature* 436: 1113-8.

Rzadzinska A, Schneider M, Noben-Trauth K, Bartles JR, Kachar B. (2002). Balanced levels of espin are critical for stereociliary growth and length maintenance. *Cell Motil Cytoskeleton* 6: 157-165.

Rzadzinska A, Schneider M, Davies C, Riordan GP, Kachar B. (2004). An actin molecular treadmill and myosins maintain stereocilia functional architecture and self-renewal. *J Cell Biol.* 164(6): 887-897.

Salles FT, Merritt Jr RC, Manor U, Dougherty GW, Sousa AD, Moore JE, Yengo CM, Dosé AC, Kachar B. (2009). Myosin IIIa boosts elongation of stereocilia by transporting espin 1 to the plus ends of actin filaments. *Nat Cell Biol.* 11(4), 443-450.

Schneider ME, Dosé AC, Salles FT, Chang W, Erickson FL, Burnside B, Kachar B. (2006). A new compartment at stereocilia tips defined by spatial and temporal patterns of myosin IIIa expression. *J. Neurosci.* 26, 10243-10252.

Sellers JR. (1999) *Myosins*, 2nd Ed. Oxford University Press, Oxford, UK.

Sells MA and Chernoff J (1997). Emerging from the PAK: the p21-activated protein kinase family, *Trends Cell Biol* 7: 162-167.

Trybus KM., Waller GS, Chatman TA. (1994). Coupling of ATPase activity and motility in smooth muscle myosin is mediated by the regulatory light chain. *J Cell Biol*. 124: 963-969.

Umeki N, Jung HS, Watanabe S, Sakai T, Li X, Ikebe R, Craig R, Ikebe M. (2009). The tail binds to the head-neck domain, inhibiting ATPase activity of myosin VIIA. *Proc Natl Acad Sci.* 106(21): 8483-8488.

Uyeda TQP, Ruppel KM and Spudich JA (1994). Enzymatic activities correlate with chimaeric substitutions at the actin-binding face of myosin. *Nature* 372: 515-518.

Vibert P, Craig R, Lehman W. (1997). Steric-model for activation of muscle thin filaments. *J Mol Biol*. 266(1): 8-14.

Virshup DM and Shenolikar S. (2009). From promiscuity to precision: protein phosphatases get a makeover. *Mol Cell*. 33(5): 537 – 545.

Waguespack J, Salles FT, Kachar B, Ricci AJ. (2007). Stepwise morphological and functional maturation of mechanotransduction in rat outer hair cells. *J Neurosci*. 27(50): 13890-13902.

Walsh T, Walsh V, Vreugde S, Hertzano R, Shahin H, Haika S, Lee MK, Kanaan M, King MC, and Avraham KB. (2002). From flies' eyes to our ears: mutations in a human class III myosin cause progressive nonsyndromic hearing loss DFNB30. *Proc Natl Acad Sci.* 99: 7518-7523.

Wes PD, Xu XZ, Li HS, Chien F, Doberstein SK, Montell C. (1999). Termination of phototransduction requires binding of the NINAC myosin III and the PDZ protein INAD. *Nat Neurosci.* 2(5):447-453.

Yengo CM and Sweeney HL (2004). Functional role of loop 2 in myosin V. *Biochemistry*. 43: 2605-2612.

Zheng L, Sekerková G, Vranich K, Tilney LG, Mugnaini E, Bartles JR. The deaf jerker mouse has a mutation in the gene encoding the espin actin-bundling proteins of hair cell stereocilia and lacks espin. *Cell* 102: 377-385.

Zhu G, Fujii K, Liu Y, Codrea V, Herrero J, and Shaw S. (2005) A single pair of acidic residues in the kinase major groove mediates strong substrate preference for P-2 or P-5 arginine in the AGC, CAMK, and STE kinase families. *J Biol Chem.* 280 (43): 36372 – 36379.

APPENDIX A

A.1 Autophosphorylation is Slow and [ATP] Dependent

One of our earliest tasks was to ascertain the rate of autophosphorylation at a constant myosin IIIa concentration and to establish useful experimental conditions for autophosphorylation treatments in future assays. We treated MIIIa 2IQ (0.5 µM) at room temperature with ATP in the concentration range of 50 µM to 2000 µM and quenched the reaction with SDS sample buffer at ten time points within 0 – 60 min of incubation. Samples were subjected to SDS-PAGE and Western blotting using antiphosphothreonine and antiphosphoserine primary antibodies (Zymed Laboratories Inc), horseradish peroxidase-linked IgG secondary antibody (Cell Signaling Technology), and Lumiglo chemiluminescence reagent (Cell Signaling Technology). Densitometry analysis using Image J software (NIH) was performed to determine relative band intensities. Membranes were stripped and reprobed with anti-FLAG antibody to detect total protein.

We found that threonine phosphorylation rates were linearly dependent on ATP concentration in the range of 50 to 1000 µM and that autophosphorylation was quite slow compared to the motor ATPase rate. While many Pak1 kinases turn over rapidly, the slow steady-state rate of the myosin IIIa kinase activity indicated that it does not turn over rapidly without phosphorylating the substrate (Wu *et al* 2003, Dosé *et al* 2006). We used these data to select an ATP concentration of 200 µM and a treatment time of one hour for further experiments, an ATP concentration at which the threonine phosphorylation rate for 0.5 µM MIIIa 2IQ was ~0.2 min^{-1} (Dosé *et al* 2006). (Appendix figure A2).

A.2 Two Residues Are Autophosphorylated Per Myosin Molecule

Time courses were performed to determine the number of target residues that become autophosphorylated, following the protocol described in A.1 but using (γ-^{32}P) ATP as the substrate. The number of moles of ^{32}P incorporated per mole of MIIIa 2IQ was determined by scintillation counting. Samples were subjected to SDS-PAGE, bands were excised and dissolved in 30% H_2O_2, and scintillation counting was conducted in conjunction with a standard curve. By comparison to the standard curve it was determined that two moles of phosphate were incorporated per mole of myosin, indicating that two phosphorylation sites are targeted during the assay (Dosé *et al* 2006). However, because we are only measuring an increase in phosphorylation it is possible that an initial level of phosphorylation is present following the expression and purification process (Dosé *et al* 2006). (Appendix figure A3). In this assay measuring total autophosphorylation (both serine and threonine target residues), the rate was approximately 2-fold slower than that determined by Western blotting for phosphothreonine incorporation. This indicates that serine phosphorylation is likely and that it most likely occurs at a slower rate than threonine phosphorylation. (Dosé *et al* 2006).

A.3 MIIIA 2IQ ΔKinase is Not Phosphorylated

We demonstrated both by Western blotting and by phosphorimaging that the kinase-deleted myosin IIIa construct cannot become phosphorylated in the presence of ATP during the kinase assay conducted as described above (Appendix Figures A4 A and B). (Dosé *et al* 2008).

A.4 Serine Autophosphorylation is Slower Than Threonine

Serine phosphorylation proved difficult to interpret due to problems in optimizing experimental conditions for the antiphosphoserine antibody. Our few clear Western blot results suggest that serine phosphorylation does increase during the kinase assay and some amount of serine phosphorylation may take place during the cell culture or protein preparation, but this line of investigation was redirected in favor of future identification of specific target residues. (Figure A5).

A.5 Glycine and Lysine Mutants

Prior to development of the K50R mutant, we attempted to inactivate the myosin IIIa kinase by creating an individual glycine to alanine point mutation at each of the three glycine residues (G34, G36, and G39) in the highly conserved glycine-rich loop of the kinase's catalytic region. This glycine triad is one of the most highly conserved regions in kinases, and contributes to the kinase's nucleotide affinity (Hemmer *et al* 1997). A review of the literature reveals that comparable point mutations in other protein kinases have had mixed results (Hemmer *et al* 1997, Hirai *et al* 2000, Ikenoue *et al* 2004). None of our mutations successfully inactivated the myosin IIIa kinase, although one (G39A) appeared to reduce the autophosphorylation rate as compared to wild type. While the K50W mutation appeared to abolish autophosphorylation, the construct consistently exhibited a very high initial level of phosphorylation that may have included motor phosphorylation, which may have contributed to its observed reduced motor ATPase activity (Appendix Figure A6).

A.6 Dephosphorylation of MIII 2IQ WT

Because our phosphorylation Western blotss suggested that the MIIIa 2IQ wt construct is already phosphorylated at a low level following protein isolation and purification prior to experimentation, we attempted to completely dephosphorylate it by phosphatase treatment, using calf intestinal phosphatase (CIP) and protein phosphatase 1 (PP1). While these treatments did remove the low levels of initial phosphorylation as detected by Western blotting with antiphosphoserine and antiphosphothreonine primary antibodies (Appendix Figure A7), the dephosphorylated protein was not detectibly different from untreated wild type in the actin-activated ATPase assay (data not shown). It is likely that this was due to rapid rephosphorylation to initial levels once ATP was added to the assay, which may involve primarily kinase rather than motor phosphorylation.

A.7 K50R Transient Kinetics

We have partially characterized the transient kinetics of the MIIIa 2IQ K50R ATPase, particularly focusing on those components of the ATPase cycle that may specifically be altered by the K50R kinase mutation, and those identified as points of difference between wild-type and kinase-deleted MIIIa 2IQ in our previous investigations (Dosé *et al* 2008).

The rates of ATP binding to the kinase domain and to the motor domain were found to be comparable in our K50R construct to those determined in our earlier characterization of MIIIa 2IQ wt (Dosé *et al* 2006) (Appendix Figure A8). Our previous characterization of MIIIa 2IQ ΔK had found it to exhibit slow, rate-limiting ATP hydrolysis and an accelerated transition between actomyosin.ADP states (Dosé *et al*

2008). However, the data we have collected thus far regarding any differences in rates of ATP hydrolysis between MIIIa 2IQ K50R and the wild type construct have been inconclusive (Appendix Figure A9). Our results indicate that the transition between the two actomyosin.ADP states is rate limiting for the K50R mutant, as it is for wild type, but the equilibrium constant governing the transition may be enhanced for K50R. (Appendix Figure A10). See Appendix Table A1 for values obtained.

A.8 Autophosphorylation Target Residues

An important issue we have attempted to address and remains an ongoing project in our lab is the identification of specific phosphorylation target residues in human myosin IIIa. As noted in A.2, two sites become autophosphorylated during incubation in the presence of ATP (Komaba *et al* 2003, Dosé *et al* 2007), and it is possible that some phosphorylation takes place during the Sf-9 cell culturing process or during protein isolation and purification. Preliminary mass spectroscopy analysis has been conducted on our myosin samples by Dr. Stanley Stevens (University of Florida Protein Core Facility), pointing to several putative autophosphorylatable sites on both the motor and the kinase that warrant further investigation (See Appendix Figure A11).

Currently we have several lines of evidence that strongly indicate kinase phosphorylation at a threonine corresponding to a phosphorylatable serine/threonine at the canonical Pak kinase activation site on the activation loop of its catalytic domain, Thr184 in the myosin IIIa kinase domain. Not only did the mass spectrometry analysis indicate phosphorylation at this residue, but the literature indicates that phosphorylation at this site is virtually a universal requirement for activation of the Pak kinases (Thr 423 in mammalian Pak1), which may be accomplished by either intermolecular

autophosphorylation or by the activity of another cellular kinase (Lei *et al* 2000, Lei *et al* 2005 review). Close correlation between the PSSM-determined "most favored" nearby residues for Pak1 kinase target specificity and the specific sequence of basic residues upstream of T184 (P -5 to P -1) as well the nearby downstream sequence also provides strong evidence for its *in vivo* phosphorylation (Rennefahrt *et al* 2007). We have cloned and infected Sf-9 cells with both T184A and T184E MIIIa 2IQ genes, and will soon begin investigations to evaluate the significance of phosphorylation at this site. It is possible that other kinase domain residues also may be targeted for phosphorylation, either for inhibition or for modulation of kinase activity.

The motor's loop 2 residue(s) targeted for autophosphorylation by the human myosin IIIa kinase does/do not appear to correspond to either of the autophosphorylation targets published for *Limulus* myosin IIIa (Cardasis *et al* 2007). Only one of the sites is a serine/threonine in human myosin IIIa, and a serine → alanine substitution did not reduce autophosphorylation as detected by antiphosphoserine Western blotting (See Figure A12). Indeed, an alignment of fish, human, *Drosophila* and *Limulus* myosin III protein sequences shows loop 2 to be relatively variable in both length and specific residues, especially when comparing vertebrate to invertebrate isoforms (Dosé *et al* 2003). Because the loop's specific charge characteristics contribute to the motor's actin affinity in certain steps of the ATPase cycle (Yengo and Sweeney 2005) variabilities at loop 2 may contribute to differences noted between the invertebrate and vertebrate myosin III motors.

Our preliminary mass spectroscopy analysis suggested threonine-886, upstream from the *Limulus* target residues, as a potential site for autophosphorylation, and

comparison with the PSSM-derived predicted surrounding residues provides reasonable support to continue with direct testing. Further verification by mass spectroscopy along with direct testing will be required to ascertain these and other potential targets and evaluate the functional effects of their autophosphorylation.

An additional site on the kinase is also highly likely to be a phosphorylation target, but could not be distinguished between serine-177 and threonine-178. This site is not a consensus target for Pak phosphorylation and may serve to modulate or inhibit kinase activity. Because we suspect that there is at least one serine targeted for phosphorylation we predict that serine-177 is more likely to be the phosphorylated target residue. However an additional mass spectroscopy analysis will be undertaken to clarify these findings.

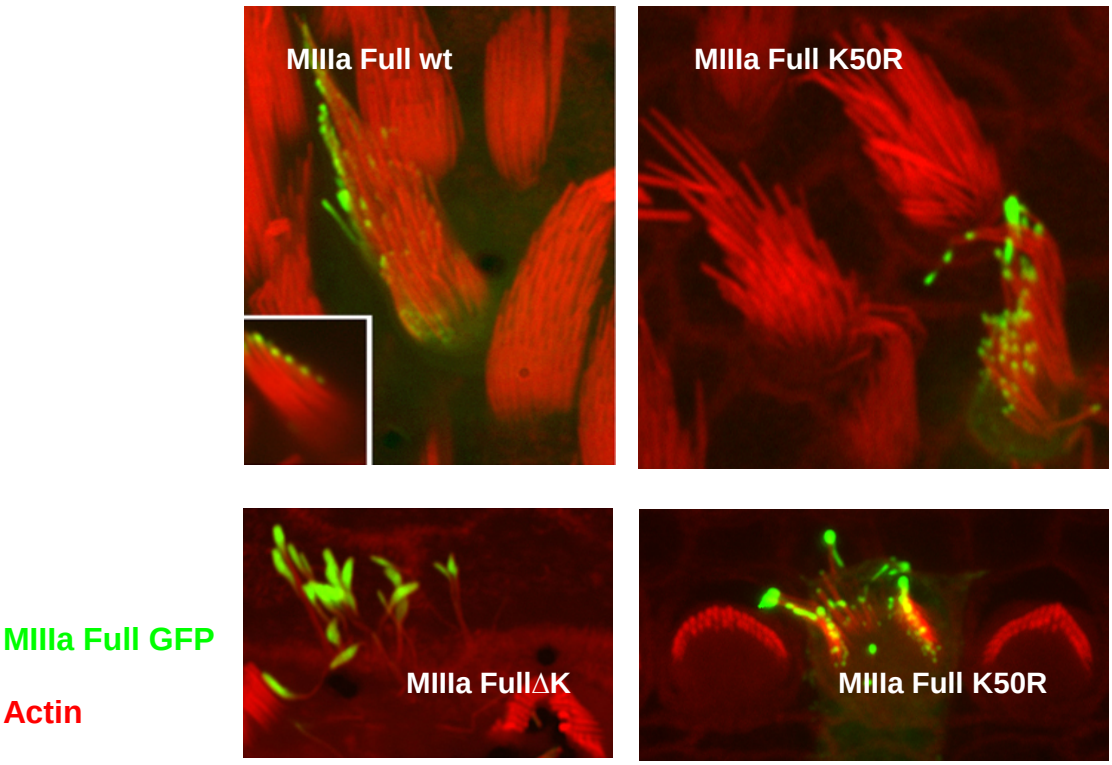

Appendix Figure A1 (Supplemental). Kinase-inactivated myosin IIIa localizes to stereocilia tips more effectively than wild-type. (From Kachar Lab, NIH). Mouse inner ear hair cells were transfected with human MIIIa full length-GFP constructs, the wild type (upper left), kinase deleted (lower left), and kinase inactivated (upper and lower right). All of the myosin constructs localized to stereocilia tips, but with variability in concentration levels. Myosin concentrations at the tips were lowest for wild type, highest for kinase deleted, and intermediate for kinase inactivated, which provides support for our *in vitro* results using the shortened (MIIIa 2IQ) myosin IIIa constructs. MIIIa is visualized with green fluorescent protein, while actin is red (rhodamine-phalloidin staining).

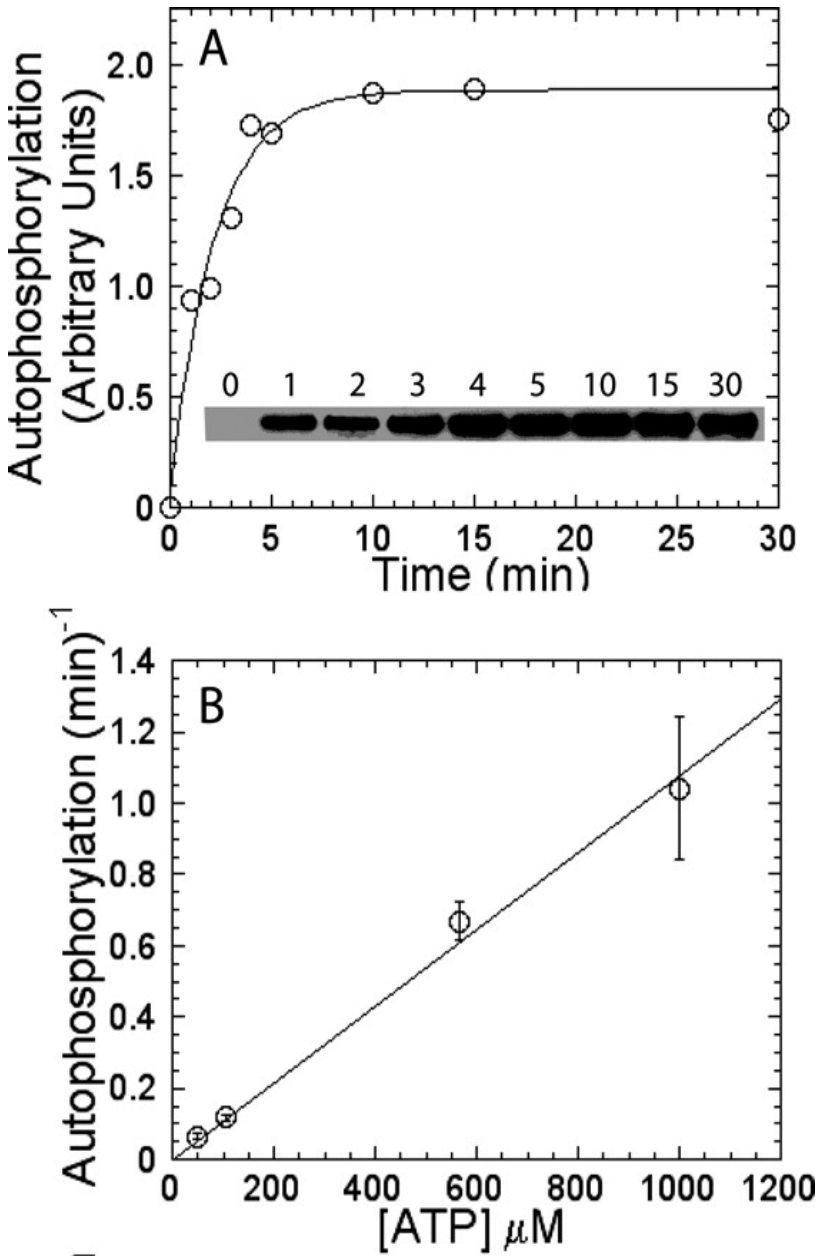

Figure A2. Rate of MIIIa 2IQ autophosphorylation was monitored by Western blotting with anti-phosphothreonine primary antibody. MIIIa 2IQ (5 μM) was incubated with ATP for 0-60 min (room temperature) and the reaction was quenched with SDS loading buffer. Increase in phosphothreonine as a function of time was analyzed using Image J software. A. Autophosphorylation time course at 565 μM ATP is shown. Data are fit to a single exponential function (k_{obs} = 0.46 ± 0.07 min^{-1} and linear phase = 0.67 ± 0.05 min^{-1}). *Inset* shows the Western blotting results (minutes of ATP incubation given). B, Initial linear phase of the time course allowed us to determine the autophosphorylation rate at each ATP concentration. The plot demonstrates that autophosphorylation rate (min^{-1}) is linearly dependent on ATP concentration in the concentration range measured (linear fit = 0.0010 ± 0.0001 $\mu M^{-1} \cdot min^{-1}$). (Dosé *et al* 2006).

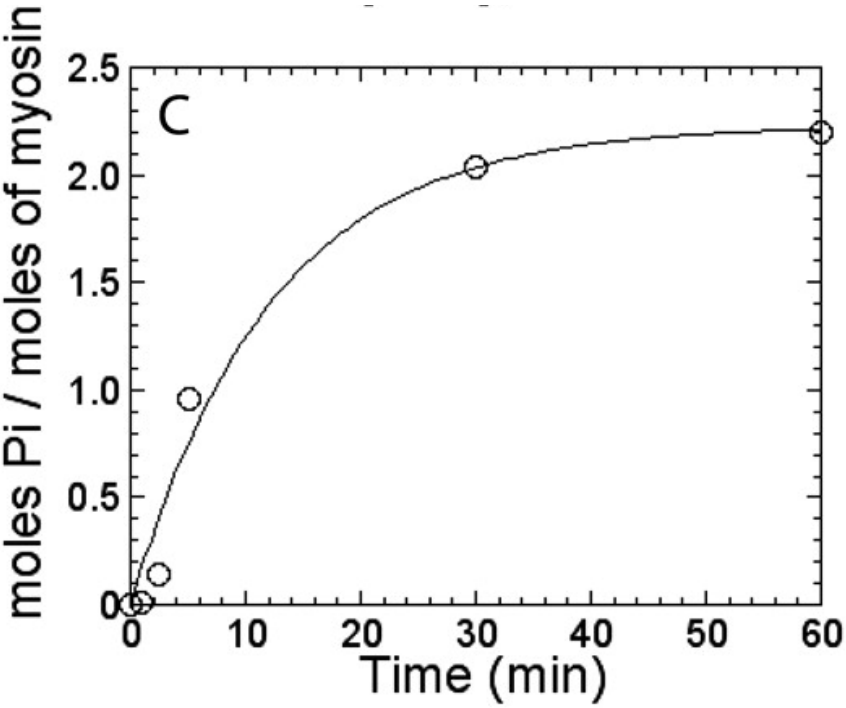

Figure A3. A time course measuring kinase activity was conducted as described earlier, using [γ-^{32}P]ATP (200 μM) to determine the total amount of phosphate incorporation at each time point. Samples were subjected to SDS-PAGE electrophoresis, bands were cut out and dissolved in 30% H_2O_2. The amount of ^{32}P incorporation as a function of time was fit to a single exponential function (k_{obs} = 0.082 ± 0.02 min^{-1}, linear phase = 0.16 ± 0.03 min^{-1}) to determine the maximum number of moles of ^{32}P per mol of myosin III (2.2 ± 0.2). (Dosé *et al* 2006).

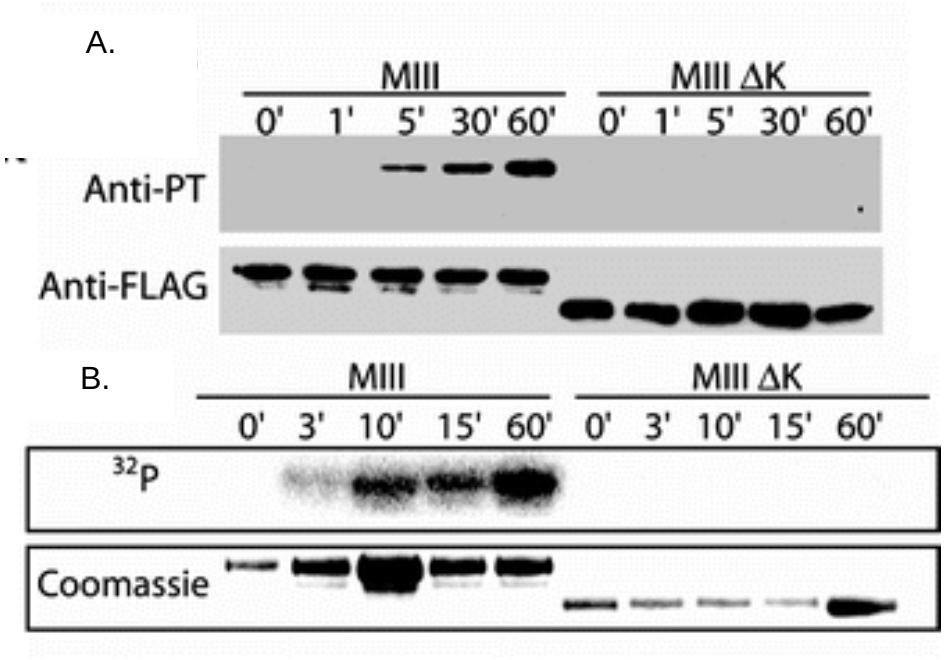

Figure A4. Western blot and phosphorimage of purified MIIIa and MIIIa ΔK autophosphorylation. (A) Anti-phosphothreonine Western blot. A time course of MIIIa autophosphorylation upon treatment with ATP demonstrates the increase in phosphothreonine content over a 60 min period (time points = 0, 1, 5, 30, and 60 min). MIIIa Δ*K* was also examined in the presence of ATP for the same time points as MIIIa. The blot was stripped and reprobed with anti-FLAG to assess equal loading of samples. (B) Phosphorimage of ^{32}P incorporation by MIIIa 2IQ and MIIIa 2IQ ΔKinase (60 minute room temperature incubation). No phosphate incorporation was noted for the kinase deleted construct within the time of the experiment (Dosé *et al* 2008).

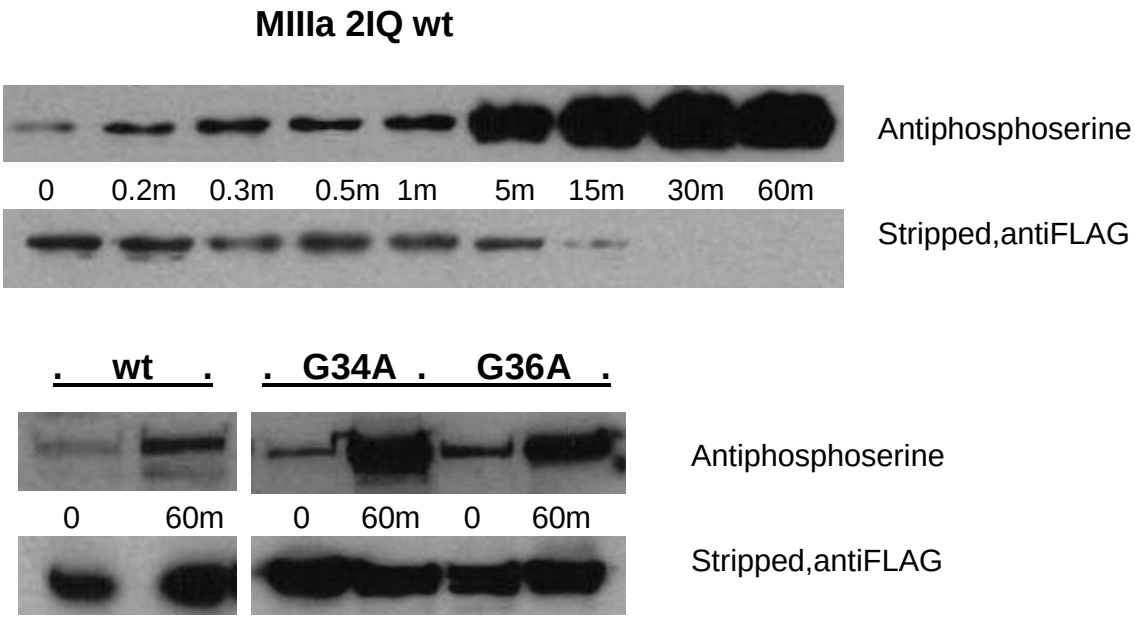

Figure A5. Western blotting indicates that autophosphorylation targets serine residue(s) as well as threonine (see Figure A2). Autophosphorylation assays were conducted as described (200 µM ATP, room temperature), using antiphosphoserine as the primary antibody. Results suggest that autophosphorylation targets for the MIIIa 2IQ kinase include both serine and threonine residues. The stripping conditions for the time course assay appear to not have been completely successful.

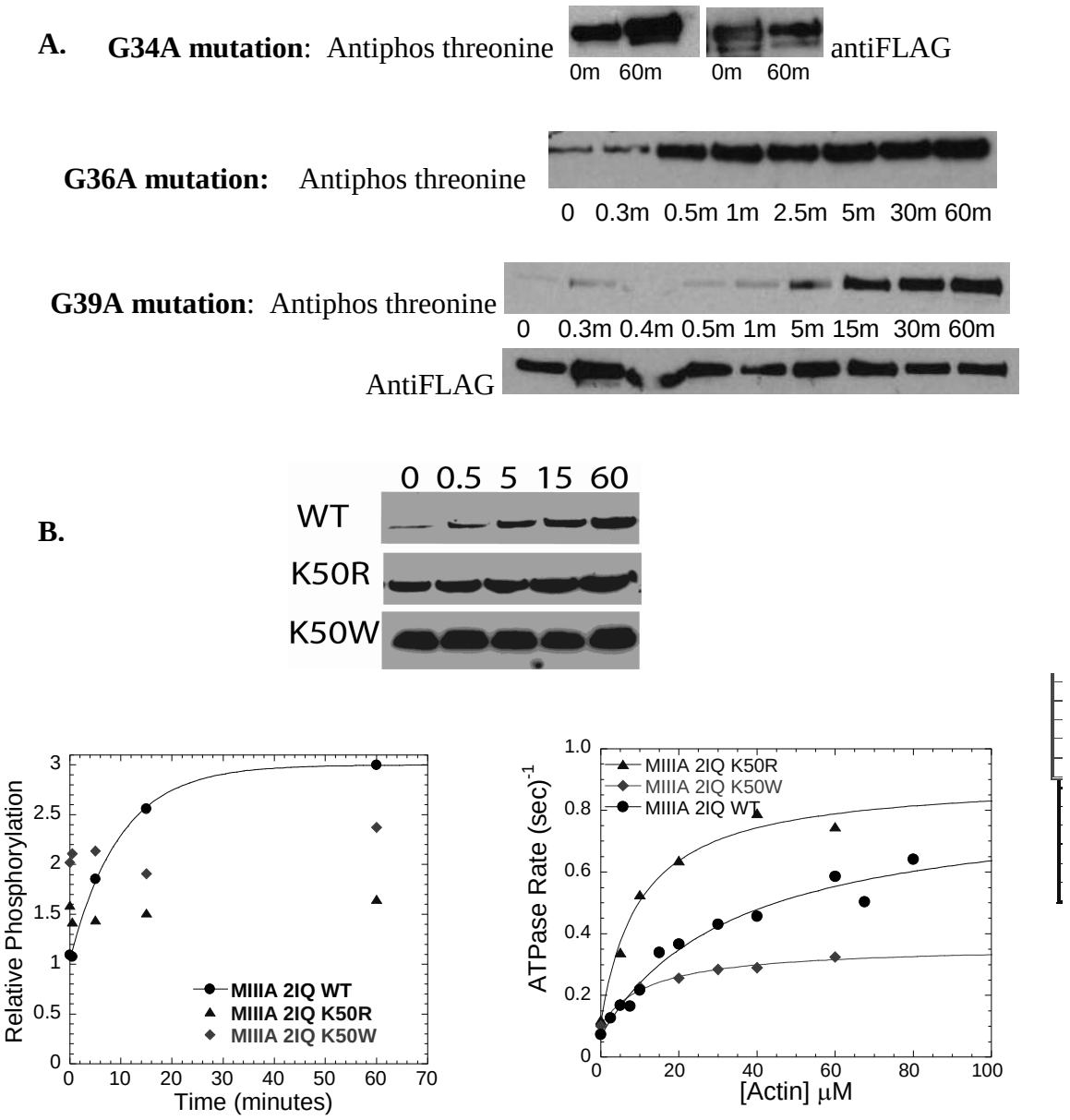

Figure A6. A. Individual point mutations in the conserved glycine loop of the MIIIa 2IQ kinase domain did not abolish autophosphorylation capability as determined by time course kinase assays (0-60m incubation with 200 μM ATP at room temperature, quenched by SDS sample buffer). B. Both K50R and K50W point mutations appeared to abolish autophosphorylation, but were accompanied by high phosphorylation from the cell culture/purification process. The very high initial phosphorylation of K50W was associated with low ATPase activity, and so may have involved motor as well as kinase phosphorylation. (See further K50R analysis in the main body of this dissertation.) All samples were resolved by SDS-PAGE electrophoresis followed by Western blotting, using antiphosphothreonine as the primary antibody. Stripped membranes were reprobed with anti-FLAG antibody to assess evenness of loading.

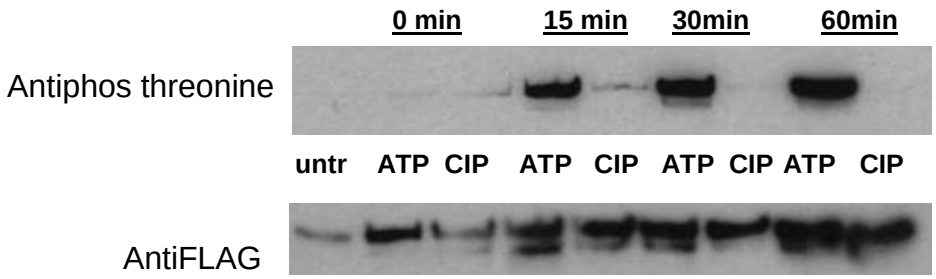

Figure A7. Treatment with calf intestinal phosphatase for 0 to 60 minutes resulted in removal of initial phosphorylation, while incubation with ATP (as described for other kinase assays) produced a progressive increase in phosphorylation comparable to other similar assays. Dephosphorylated myosin IIIa 2IQ, however, did not give evidence of differences from untreated myosin in steady-state actin-activated ATPase assays (data not included).

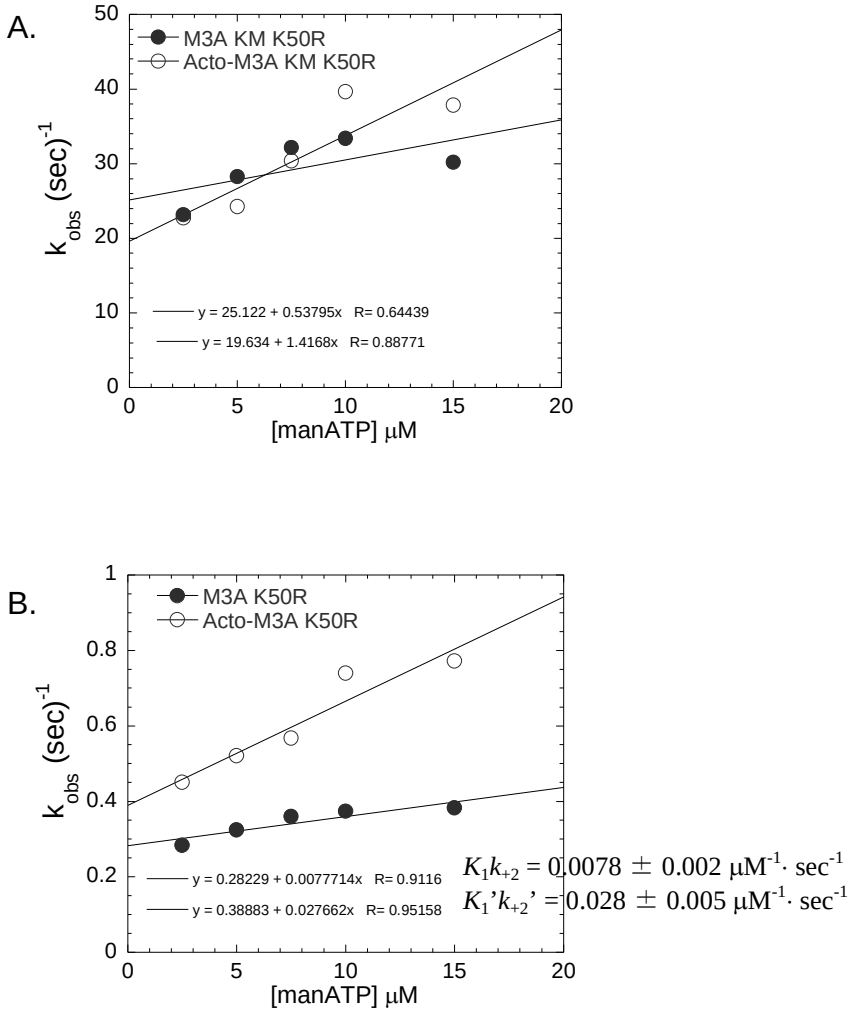

Figure A8. The rate of ATP binding for MIIIa 2IQ K50R was measured by kinetic competition with mantATP. MIII 2IQ (K50R) (1 μM) or acto-MIII 2IQ (K50R) was mixed with 5 μM mantATP and varying concentrations of ATP. The rate of the fluorescence increase was linearly dependent on ATP concentration in the presence and absence of actin. A fast and a slow phase were observed both in the presence and the absence of actin, which was interpreted as the difference between rates of ATP binding to the kinase vs. the motor domains (Dosé *et al*, 2006). A) The fast phase, corresponding to kinase binding, was fit to a single exponential function at all ATP concentrations in the absence and presence of actin. B) The slow phase, corresponding to motor binding, was fit to a single exponential function at all ATP concentrations in the absence and presence of actin. The rate of ATP binding was plotted as a function of ATP concentration to determine the equilibrium constant (K_1) and maximum rate of ATP binding (k_{+2}).

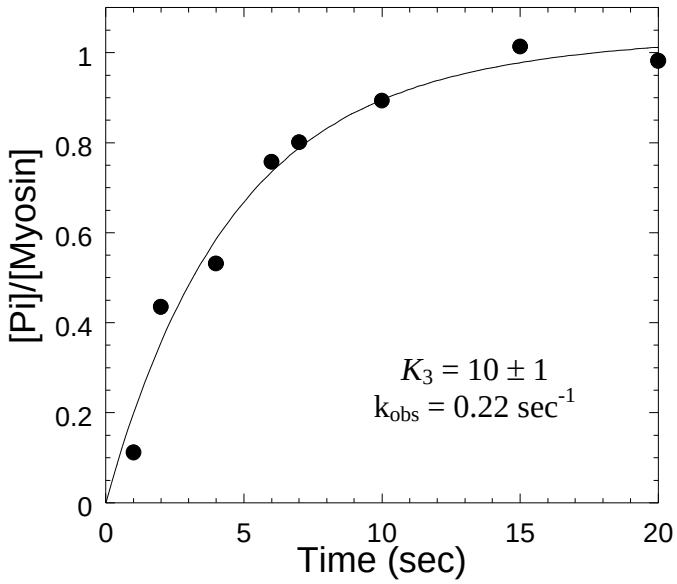

Figure A9. The MIIIa 2IQ K50R equilibrium constant for ATP hydrolysis determined by acid quench experiments. MIIIa 2IQ K50R (1.0 μM) was mixed with [γ-^{32}P]-ATP (100μM) and allowed to age for specific time points (1-20 seconds) before manually quenching the reaction with acid. The amount of ^{32}P and thus the amount of ATP hydrolyzed was determined by scintillation counting. The data was fit to a single exponential function ($k_{obs} = 0.22\ sec^{-1}$) with a steady state rate ($0.01\ sec^{-1}$) and a burst of 0.97 μM P_i per μM MIIIa 2IQ K50R. The maximum rate of ATP hydrolysis was determined by kinetic simulation ($k_{+3} + k_{-3} \geq 1.0\ sec^{-1}$). Further experimentation is required before a conclusive comparison may be made between ATP hydrolysis rates for this construct and MIIIa 2IQ wild type.

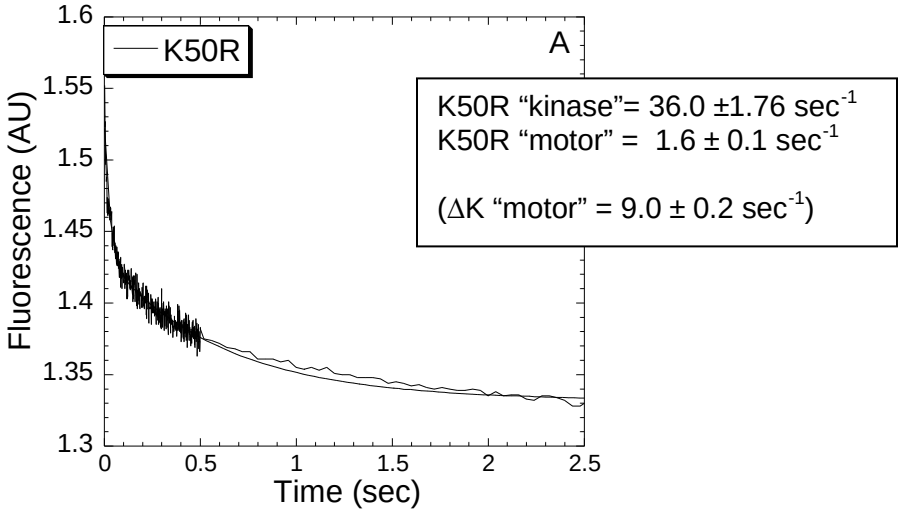

Figure A10. The rate of mantADP release following binding to actin in the M.ADP.Pi state. MIIIa 2IQ K50R (1 μM) (2.25 μM) was mixed with 12.5 μM mantATP, aged for 4 seconds and then mixed with 20 μM actin and 0.5 mM ADP (final reaction conditions: 0.5 or 1.13 μM MIIIa 2IQ, 6.25 μM mantATP, 20 μM actin, and 0.5 mM ADP). The mant fluorescence transients were fit to a two exponential function for MIIIa 2IQ (K50R) representing ADP release from the kinase and motor domains. Results are contrasted with those previously obtained for MIIIa 2IQ ΔK (ADP release from the motor domain only), which fit to a single exponential function (Dosé *et al* 2008).

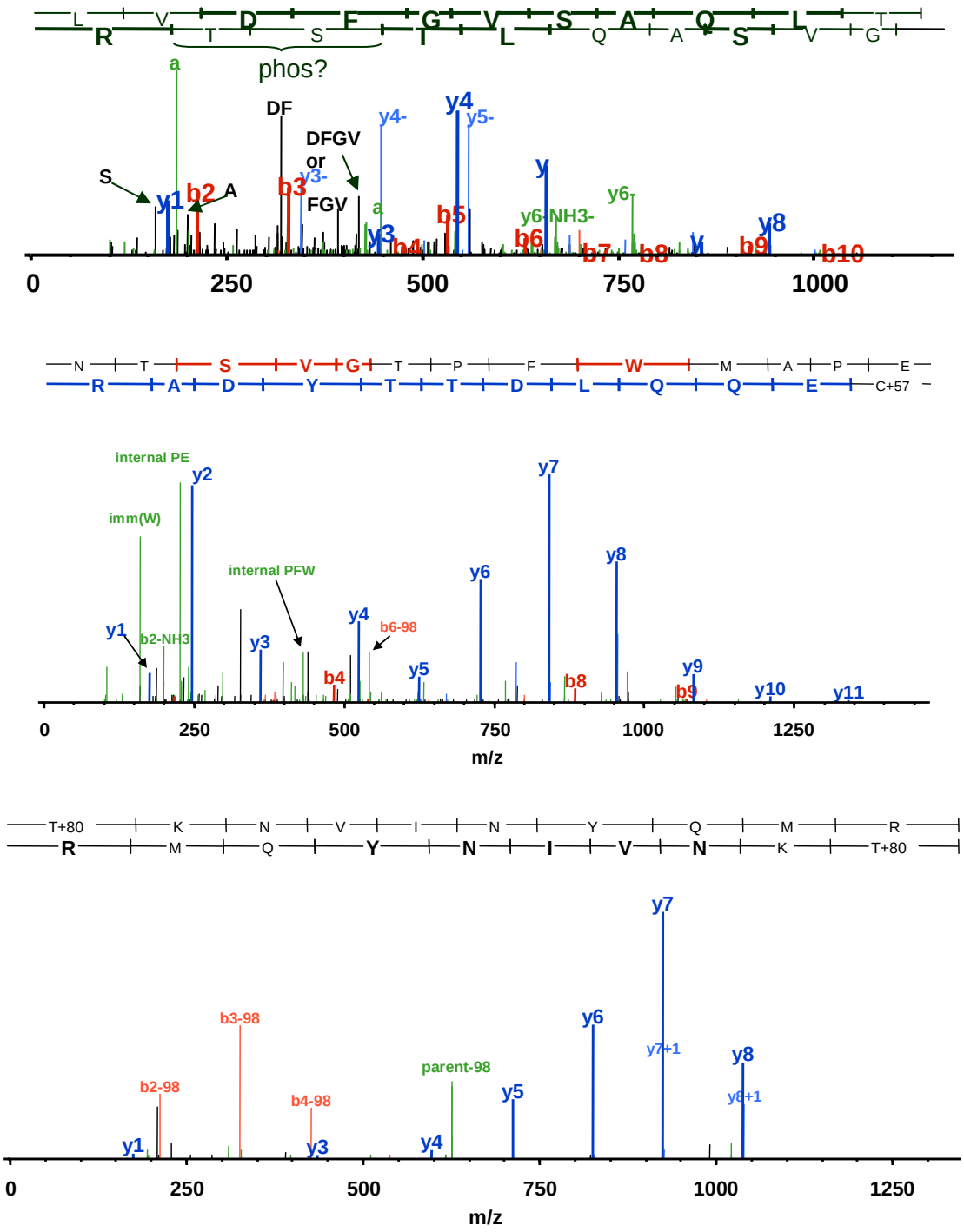

Figure 11. Mass spectroscopy reports mapping potential phosphorylation target residues in myosin IIIa. Each of the above reports maps one of the three putative phosphorylatable residues identified in myosin IIIa samples submitted for analysis. These sites were mapped to S177/T178, T184 and T886 respectively. (Dr. Stanley Stevens, University of Florida Core Protein Facility).

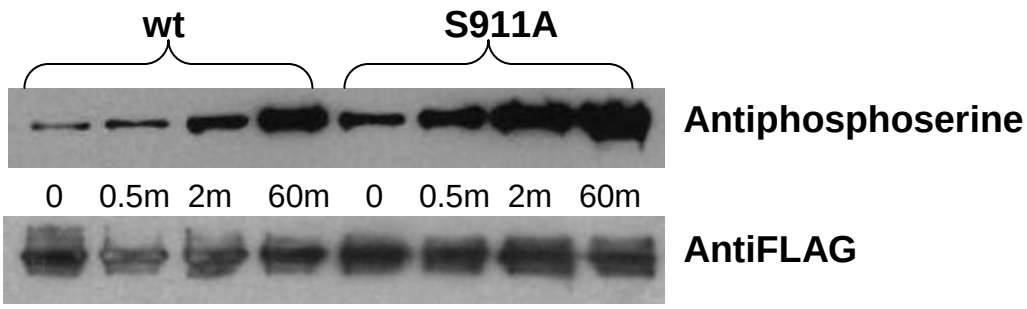

Figure A12. The point mutation S911A in loop 2 of the human myosin IIIa motor did not block serine autophosphorylation. The band intensity difference between 0 and 60 minutes was similar for S911A construct and wild type.

Table A1. Summary of rate and equilibrium constants in the myosin IIIA motor ATPase cycle.

ATP Binding and Hydrolysis

Rate/Equilibrium Constant	MIII	MIII ΔK	MIII K50R (y-int)
[a] K_1k_{+2} ($\mu M^{-1}\cdot sec^{-1}$)	0.010 ± 0.004	0.031 ± 0.005	0.0078 ± 0.002 (0.28±0.02)
[b] K_1k_{+2} ($\mu M^{-1}\cdot sec^{-1}$)	0.002 ± 0.001	0.075 ± 0.005	N/A
[c] K_3	9	1.5	
[a] $K'_1k'_{+2}$($\mu M^{-1}\cdot sec^{-1}$)	0.005 ± 0.002	0.116 ± 0.013	0.028 ± 0.005 (0.39±0.05)
[b] $K'_1k'_{+2}$ ($\mu M^{-1}\cdot sec^{-1}$)	0.043 ± 0.010	0.099 ± 0.005	N/A
[d] $K'_1k'_{+2}$ ($\mu M^{-1}\cdot sec^{-1}$)	0.022 ± 0.001	0.054 ± 0.005	0.066 ± 0.01
[d] $1/K'_1$ (μM)	11,144 ± 2,319	4,591 ± 1,063	5,016 ± 697
[d] k'_{+2}(sec^{-1})	246 ± 38	248 ± 34	269 ± 19

ADP Binding

[e] k'_{+5B} (sec^{-1})	6.8 ± 0.2	6.5 ± 0.1	4.69 ± 0.8 light scatter
[e] k'_{-5B}($\mu M^{-1}\cdot sec^{-1}$)	1.0 ± 0.1	0.4 ± 0.1	0.2
[e] K'_{5B} (μM)	6.8 ± 0.4	16.4 ± 2.2	23.6 ± 5.9
[e] $*k'_{+5A}$ (sec^{-1})	0.60 ± 0.10	0.67 ± 0.20	0.81 ± 0.18 light scatter
[f] $*k'_{+5A}$ (sec^{-1})	0.97 ± 0.03	0.62 ± 0.07	0.58 ± 0.023
[f] $*k'_{-5A}$ (sec^{-1})	0.54 ± 0.08	0.50 ± 0.10	0.15 ± 0.07
[f] $*K'_{5A}$	1.8 ± 0.3	1.2 ± 0.3	3.86
[f] k'_{+5B} (sec^{-1})	9.84 ± 0.25	8.5 ± 0.4	6.1 ± 0.3
[f] k'_{-5B} ($\mu M^{-1}\cdot sec^{-1}$)	0.29 ± 0.11	0.29 ± 0.07	0.55 ± 0.49
[f] K'_{5B}(μM)	34 ± 14	29.1 ± 7.3	11.09
[f] k_{+5A} (sec^{-1})	1.00 ± 0.24	0.45 ± 0.09	0.05 ± 0.063
[f] k_{-5A} (sec^{-1})	0.88 ± 0.11	0.35 ± 0.10	0.89 ± 0.06
[f] K_{5A}	1.1 ± 0.3	1.2 ± 0.4	0.73
[f] k_{+5B} (sec^{-1})	9.26 ± 1.55	4.8 ± 1.3	10.11 ± 0.89
[f] k_{-5B} ($\mu M^{-1}\cdot sec^{-1}$)	0.31 ± 0.09	0.51 ± 0.12	0.14 ± 0.06
[f] K_{5B} (μM)	30 ± 11	9.4 ± 3.4	71.42

Actin Binding

[h] k_{+6} ($\mu M^{-1}\cdot sec^{-1}$)	11.4 ± 0.4	21.2 ± 0.4	10.4 ± 1.22
[h] k_{-6} (sec^{-1})	1.5 ± 0.1	0.40 ± 0.02	55 ± 4
[h] $1/K_6$ (μM)	0.13 ± 0.01	0.020 ± 0.001	
[h] k_{+10A} ($\mu M^{-1}\cdot sec^{-1}$)	14.6 ± 0.6	16.8 ± 0.4	*Dominated by slow phase*
[h] k_{-10A} (sec^{-1})	1.2 ± 0.1	0.30 ± 0.01	
[h] $1/K_{10B}$ (μM)	0.08 ± 0.01	0.020 ± 0.001	
[h] k_{+10A} ($\mu M^{-1}\cdot sec^{-1}$)	NA	1.1 ± 0.1	0.13 ± 0.010 0.08 ± 0.033
[h] k_{-10A} (sec^{-1})	NA	1.1 ± 0.1	
[h] $1/K_{10A}$ (μM)	NA	1.0 ± 0.1	
[i] $1/K_{10A}$ (μM)	5.0		

Note: see next page for legend.

[a] mantATP fluorescence
[b] ATP binding by competition with mantATP
[c] Acid quench with [^{32}P]ATP
[d] ATP-induced dissociation monitored by light scatter
[e] ADP competition with ATP-induced dissociation monitored by light scatter or pyrene actin
[f] mantADP fluorescence
[g]Phosphate binding protein
[h]Pyrene actin fluorescence
[i]Predicted from kinetic simulation
*Note the rate and equilibrium constants defining K'_{5A} were modeled with an off-pathway intermediate in MIII ΔK.